Identification of SARS-CoV-2-specific immune alterations in acutely ill patients

Rose-Marie Rebillard, Marc Charabati, Camille Grasmuck, Abdelali Filali-Mouhim, Olivier Tastet, Nathalie Brassard, Audrey Daigneault, Lyne Bourbonniere, Sai Priya Anand, Renaud Balthazard, et al.

JCI The Journal of Clinical Investigation

Identification of SARS-CoV-2–specific immune alterations in acutely ill patients

Rose-Marie Rébillard, … , Alexandre Prat, Catherine Larochelle

J Clin Invest. 2021;131(8):e145853. https://doi.org/10.1172/JCI145853.

Research Article COVID-19

Graphical abstract

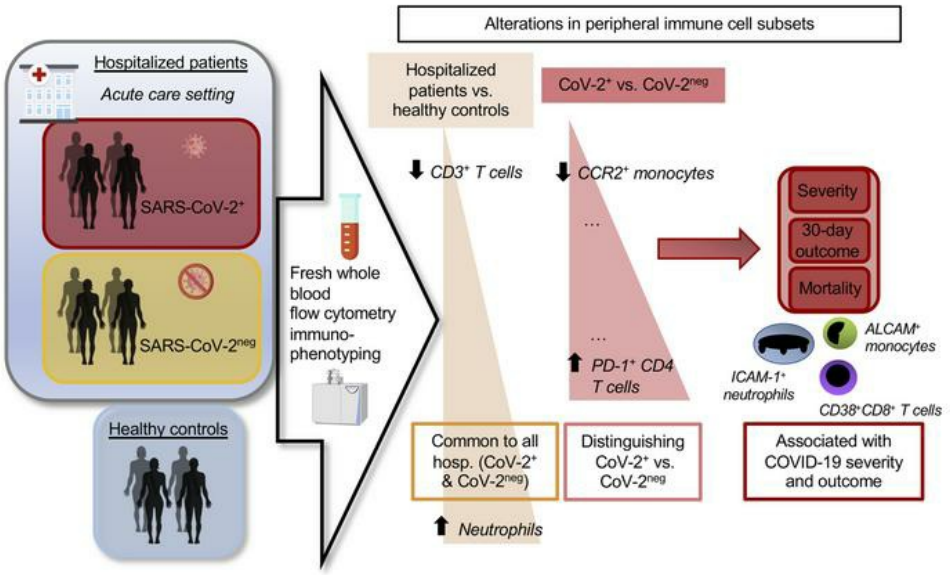

Identification of SARS-CoV-2–specific immune alterations in acutely ill patients

Rose-Marie Rébillard,[1,2] Marc Charabati,[1,2] Camille Grasmuck,[1,2] Abdelali Filali-Mouhim,[2] Olivier Tastet,[2] Nathalie Brassard,[2] Audrey Daigneault,[2] Lyne Bourbonnière,[2] Sai Priya Anand,[2,3] Renaud Balthazard,[1,2] Guillaume Beaudoin-Bussières,[2,4] Romain Gasser,[2,4] Mehdi Benlarbi,[2,4] Ana Carmena Moratalla,[1,2] Yves Carpentier Solorio,[1,2] Marianne Boutin,[2,4] Negar Farzam-kia,[1,2] Jade Descôteaux-Dinelle,[2,4] Antoine Philippe Fournier,[1,2] Elizabeth Gowing,[1,2] Annemarie Laumaea,[2,4] Hélène Jamann,[1,2] Boaz Lahav,[2] Guillaume Goyette,[2] Florent Lemaître,[1,2] Victoria Hannah Mamane,[1,2] Jérémie Prévost,[2,4] Jonathan Richard,[2,4] Karine Thai,[1,2] Jean-François Cailhier,[2,5] Nicolas Chomont,[2,4] Andrés Finzi,[2,3,4] Michaël Chassé,[2,5] Madeleine Durand,[2,5] Nathalie Arbour,[1,2] Daniel E. Kaufmann,[2,5] Alexandre Prat,[1,2] and Catherine Larochelle[1,2]

[1]Department of Neuroscience, Université de Montréal, Montreal, Quebec, Canada. [2]Centre de recherche du Centre hospitalier de l'Université de Montréal (CRCHUM), Montreal, Quebec, Canada. [3]Department of Microbiology and Immunology, McGill University, Montreal, Quebec, Canada. [4]Department of Microbiology, Infectious Diseases and Immunology, and [5]Department of Medicine, Université de Montréal, Montreal, Quebec, Canada.

Dysregulated immune profiles have been described in symptomatic patients infected with SARS-CoV-2. Whether the reported immune alterations are specific to SARS-CoV-2 infection or also triggered by other acute illnesses remains unclear. We performed flow cytometry analysis on fresh peripheral blood from a consecutive cohort of (a) patients hospitalized with acute SARS-CoV-2 infection, (b) patients of comparable age and sex hospitalized for another acute disease (SARS-CoV-2 negative), and (c) healthy controls. Using both data-driven and hypothesis-driven analyses, we found several dysregulations in immune cell subsets (e.g., decreased proportion of T cells) that were similarly associated with acute SARS-CoV-2 infection and non–COVID-19-related acute illnesses. In contrast, we identified specific differences in myeloid and lymphocyte subsets that were associated with SARS-CoV-2 status (e.g., elevated proportion of ICAM-1$^+$ mature/activated neutrophils, ALCAM$^+$ monocytes, and CD38$^+$CD8$^+$ T cells). A subset of SARS-CoV-2–specific immune alterations correlated with disease severity, disease outcome at 30 days, and mortality. Our data provide an understanding of the immune dysregulation specifically associated with SARS-CoV-2 infection among acute care hospitalized patients. Our study lays the foundation for the development of specific biomarkers to stratify SARS-CoV-2–positive patients at risk of unfavorable outcomes and to uncover candidate molecules to investigate from a therapeutic perspective.

Introduction

SARS coronavirus 2 (SARS-CoV-2), which causes coronavirus disease 2019 (COVID-19), has now infected millions of people worldwide and caused the death of over 2 million patients (WHO operational update; https://covid19.who.int/, accessed on January 18, 2021). The spectrum of clinical mani festations in patients infected with SARS-CoV-2 (SARS-CoV-2$^+$) ranges from asymptomatic to severe acute respiratory distress syndrome (ARDS) and multiple organ involvement (1). Increasing evidence supports that the immune reaction plays a central role in COVID-19 severity and outcome. Therefore, it is essential to understand immune responses generated in COVID-19 to stratify patients at higher risk of unfavorable outcomes and identify novel therapeutic targets. Several risk factors for negative clinical outcomes have been identified (2, 3), but the underlying mechanisms of effective versus impaired/deleterious immune responses to SARS-CoV-2 remain unclear.

Age is the greatest risk factor for COVID-19 severity and mortality (2–6). Obesity and cardiovascular comorbidities, such as high blood pressure and diabetes, also significantly increase the risk of severe clinical course in individuals infected with SARS-CoV-2 (3, 4, 6, 7). Notably, each of these risk factors — age, obesity, diabetes, and cardiovascular comorbidities — is associated with alterations in immune responses and a state of chronic low-grade inflammation (8–10) that could contribute to the elevated morbidity and mortality in COVID-19, as in other infectious conditions (11–13). Dysregulations of the immune profile in hospitalized patients infected with SARS-CoV-2 include elevated levels of circulating IL-6 and decreased peripheral lymphocyte/neutrophil ratio, which are predictive of worse clinical outcomes (7, 14, 15). Accumulating evidence suggests that both hyperactivation and exhaustion of different T and B cell subsets characterize COVID-19 (7, 14, 16). A state of activation of CD4$^+$ T cells with an increased CD4$^+$/CD8$^+$ ratio has been recently linked to disease severity (14, 17). Whether the reported immune alterations

Authorship note: RMB, MC, and CG are co–first authors and contributed equally to this work.
Conflict of interest: The authors have declared that no conflict of interest exists.

Submitted: November 17, 2020; **Accepted:** February 19, 2021;
Published: April 15, 2021.
Reference information: *J Clin Invest*. 2021;131(8):e145853.
https://doi.org/10.1172/JCI145853.

Table 1. Baseline characteristics of populations

Baseline clinical characteristics	Healthy controls (*n* = 49)	Hospitalized SARS-CoV-2⁻ (*n* = 22)	Hospitalized SARS-CoV-2⁺ (*n* = 50)	Statistical analysis (SARS-CoV-2⁻ vs. SARS-CoV2⁺)
Age, mean years (SD)	38.7 (11.9)	58.4 (17.2)	59.5 (14.6)	*P* = 0.9347[A]
Male sex, *n* (%)	20 (40.8)	15 (68.2)	30 (60.0)	*P* = 0.6022[B]
<60 y.o., *n* (%)	49/49 (100)	9/22 (40.9)	20/50 (40)	*P* > 0.9999[B]
Comorbidities and past medical history				
BMI over 25.0, *n* (%)	12/33 (36.4)	13/22 (59.1)	38/46 (82.6)	*P* = 0.0698[B]
Chronic renal insufficiency, *n* (%)	ND	1/22 (4.5)	11/50 (22.0)	*P* = 0.0904[B]
Cardiac condition, *n* (%)	ND	5/22 (22.7)	9/50 (18.0)	*P* = 0.7485[B]
Respiratory condition, *n* (%)	ND	7/22 (31.8)	7/50 (14.0)	*P* = 0.1073[B]
Hepatic condition, *n* (%)	ND	3/22 (13.6)	1/50 (2.0)	*P* = 0.0820[B]
High blood pressure, *n* (%)	ND	11/22 (50.0)	33/50 (66.0)	*P* = 0.2939[B]
Dyslipidemia, *n* (%)	ND	7/22 (31.8)	22/50 (44.0)	*P* = 0.4362[B]
Diabetes type 1, *n* (%)	ND	0/22 (0)	1/50 (2.0)	*P* > 0.9999[B]
Diabetes type 2, *n* (%)	ND	6/22 (27.2)	24/50 (48.0)	*P* = 0.1242[B]
Comorbidities total, *n* (excluding obesity) (%)	ND	0: 6/22 (27.2); 1–2: 9/22 (40.9); ≥3: 7/22 (31.8)	0: 11/50 (22.0); 1–2: 17/50 (34.0); ≥3: 22/50 (44.0)	*P* = 0.6235[C]
Organ transplant, *n* (%)	ND	3/22 (13.6)	4/50 (8.0)	*P* = 0.6678[B]
Active cancer, *n* (%)	ND	3/22 (13.6)	3/50 (6.0)	*P* = 0.3612[B]
Cancer history, *n* (%)	ND	4/22 (18.2)	4/50 (8.0)	*P* = 0.2372[B]
Active infection except COVID-19, *n* (%)	0/49	10/22 (45.5)	16/50 (32.0)	*P* = 0.2979[B]

[A]Mann-Whitney *U* test. [B]Fisher's exact test. [C]χ^2 test. SD, standard deviation; *n*, number of patients in specified category; ND, not determined; y.o., years old.

are specific to SARS-CoV-2 infection or commonly triggered by a range of acute illnesses, especially in older patients with preexisting medical conditions, remains unknown. We performed a detailed characterization of circulating innate and adaptive immune cells from 50 SARS-CoV-2⁺ patients (47 hospitalized in our center for COVID-19, 3 for nosocomial infections without overt respiratory symptoms) in comparison with 22 patients who were similar in regards to sex and age and hospitalized for other acute illnesses (SARS-CoV-2⁻) and 49 healthy controls (HCs). We found a SARS-CoV-2–specific immune profile that could identify relevant therapeutic targets related to severity and outcome in patients with COVID-19.

Results

SARS-CoV-2⁺ and SARS-CoV-2⁻ groups of hospitalized patients have similar prevalence of comorbidities, severity of disease, and outcome at 30 days. To investigate SARS-CoV-2–triggered alterations in the peripheral immune system, we performed extensive immune profiling of whole blood obtained from hospitalized patients and HCs. Inclusion criteria for hospitalized participants included a nasopharyngeal swab SARS-CoV-2 PCR test conducted because of symptoms compatible with COVID-19 or because participants were considered at risk of acute SARS-CoV-2 infection. Patients were classified as SARS-CoV-2⁺ patients or SARS-CoV-2⁻ patients based on the test results. Mean age and sex ratio were similar in SARS-CoV-2⁺ and SARS-CoV-2⁻ hospitalized patients' groups, whereas HCs were younger and included a higher proportion of women (Table 1). No significant differences were observed in numbers of comorbidities, history of cancer, or organ transplant between the SARS-CoV-2⁺ and SARS-CoV-2⁻ hospitalized patients (Table 1). Most hospitalized patients presented at least 1 comorbidity regardless of SARS-CoV-2 status. A greater proportion of SARS-CoV-2⁺ patients had comorbidities associated with risk for severe COVID-19 (obesity, chronic renal insufficiency, and type 2 diabetes) compared with SARS-CoV-2⁻ patients, without reaching significance (Table 1). In contrast, respiratory and hepatic conditions were more frequent among SARS-CoV-2⁻ patients (not significant), probably reflecting the patient population in our hospital.

SARS-CoV-2⁺ and SARS-CoV-2⁻ hospitalized patient groups exhibited comparable outcomes at 30 days, mortality rate, and need for invasive ventilation during hospitalization (Table 2). Acute renal insufficiency was more frequent in SARS-CoV-2⁺ patients but did not reach significance. As previously reported (2, 3, 18), SARS-CoV-2 infection was associated with a high incidence of respiratory insufficiency and encephalopathy (delirium) in hospitalized patients. The total burden of medical complications during hospitalization and the average duration of invasive ventilation were elevated in SARS-CoV-2⁺ patients (Table 2). Of note, at the time of baseline blood sampling, both groups of patients showed a similar proportion of intensive care unit (ICU) hospitalization and number of days in the hospital (Supplemental Table 1; supplemental material available online with this article; https://doi.org/10.1172/JCI145853DS1). A majority (80%) of baseline samples from SARS-CoV-2⁺ individuals harbored anti-Spike antibodies, with anti-RBD IgA, IgM, IgG, and neutralizing antibodies (NAbs) above the positivity threshold found in 80%, 66%, 70%, and 68% of patients, respectively (Table 3). In line with previous studies, levels of IgG and NAbs tended to be higher in severe COVID-19 (19, 20). At this relatively early time point, levels of NAbs were also higher in the younger patients without reaching statistical significance. Association analyses among clinical parameters (Figure 1) demonstrated that our 2 patient groups presented the expected relationships

Table 2. Clinical data related to hospitalization in SARS-CoV2⁻ and SARS-CoV-2⁺ patients

Clinical data — Hospitalization	SARS-CoV-2⁻ (*n* = 22)	SARS-CoV-2⁺ (*n* = 50)	Statistical analysis
Outcome and severity			
Symptomatic COVID-19, *n* (%)	NA	47/50 (94)	NA
Severe disease (high-flow or invasive ventilation), *n* (%)	14/22 (63.6)	21/50 (42)	*P* = 0.1255[A]
<60 y.o. in mild-moderate disease, *n* (%)	3/8 (37.5)	12/29 (41.4)	*P* > 0.9999[A]
<60 y.o. in severe disease, *n* (%)	6/14 (42.9)	8/21 (38.1)	*P* > 0.9999[A]
30-day outcome (NIH 8-point scale), mean (SD)	6.3 (2.3)	5.7 (2.5)	*P* = 0.3724[A]
30-day outcome: ambulatory (7–8 on NIH 8-point scale), *n* (%)	16/22 (72.7)	27/50 (54.0)	*P* = 0.1930[A]
30-day outcome: unfavorable (1–4 on NIH 8-point scale), *n* (%)	5/22 (22.7)	14/50 (28)	P = 0.7751A
<60 y.o. in 30-day outcome: unfavorable, *n* (%)	2/5 (40)	3/14 (21.4)	P = 0.5696A
30-day outcome: deceased, *n* (%)	2/22 (9.1)	3/50 (6.0)	P = 0.6379A
60-day outcome: deceased, *n* (%)	2/22 (9.1)	7/50 (14.0)	P = 0.7125A
Invasive ventilation during hospitalization, *n* (%)	10/22 (45.5)	21/50 (42.0)	P = 0.8017A
Total duration of invasive ventilation, median day (range)	4.5 (1–20)	24.5 (8–57)	P < 0.0001B
Medical complications during hospitalization			
Thromboembolic event excluding admission for NSTEMI, *n* (%)	2/22 (9.1)	7/50 (14.0)	*P* = 0.7125[A]
Acute renal insufficiency, *n* (%)	3/22 (13.6)	18/50 (36.0)	*P* = 0.0896[A]
Cardiac event, *n* (%)	5/22 (22.7)	12/50 (24.0)	*P* > 0.9999[A]
Respiratory insufficiency, *n* (%)	9/22 (40.9)	31/50 (62.0)	*P* = 0.1251[A]
Elevated liver enzymes, *n* (%)	8/22 (36.4)	23/50 (46.0)	*P* = 0.6061[A]
Delirium, *n* (%)	2/22 (9.1)	20/50 (40.0)	*P* = 0.0115[A]
Complications total, *n* (%)	0: 5/22 (22.7); 1–2: 14/22 (63.6); ≥3: 3/22 (13.6)	0: 12/50 (24.0); 1–2: 14/50 (28.0); ≥3: 24/50 (48.0)	*P* = 0.0074[C]

[A]Fisher's exact test. [B]Mann-Whitney *U* test. [C]χ^2 test. *n*, number of patients in specified category; y.o., years old; NA, not applicable.

between age, comorbidities (past medical history), and medical complications. Moreover, risk of death correlated with mechanical ventilation, respiratory insufficiency, and other medical complications. We also observed the expected association of SARS-CoV-2 status with typical COVID-19 symptoms at admission, as well as with delirium and respiratory insufficiency. Age, disease severity, and unfavorable outcomes were associated, but the overlap was only partial (Table 2).

Dysregulation of peripheral immune cell subsets in SARS-CoV-2⁺ and SARS-CoV-2⁻ hospitalized patients. To compare the immune profiles of SARS-CoV-2⁺ and SARS-CoV-2⁻ hospitalized patients and HCs, we performed 3 complementary flow cytometry staining panels on fresh whole blood samples and assessed the frequency of multiple subpopulations of lymphocytes, monocytes, DCs, and granulocytes. Our quality control analysis on the first 20 samples acquired in 4 batches over 2 weeks ruled out significant batch effects and validated the capture of reproducible interindividual variation (example IgD detection, Figure 2A). We used 2 analytical approaches: (a) a data-driven approach using the PhenoGraph (21) and FlowSOM (22) algorithms to cluster similar cells (Figure 2, B–D), and (b) a hypothesis-driven analysis with a conventional manual gating strategy. Overall, our analysis focused on cell subsets representing at least 1% of major cell subsets. Using the data-driven approach, we identified 21 cell clusters in the monocyte and neutrophil gate (gating according to granularity and size excluding lymphocytes, 14 markers) for the first staining panel (S1; Figure 2, B and E, and Supplemental Figure 1A), 31 cell clusters in the monocyte and lymphocyte gates for the DC/NK cell–oriented panel (S2, 14 markers, gating excluding granulocytes) (Figure 2, C and F, and Supplemental Figure 1A), and 18 cell clusters in the monocyte and lymphocyte gate for the lymphocyte-oriented panel (S3, 13 markers, gating excluding granulocytes; Figure 2, D and G, and Supplemental Figure 1A). The distribution of clustered populations, as illustrated by the uniform manifold approximation and projection (UMAP) algorithm, shows distinct populations and relative abundance of these subsets in blood samples.

We compared the abundance of these 70 identified cell clusters in the 3 donor groups: HCs, SARS-CoV-2⁺ hospitalized patients, and SARS-CoV-2⁻ hospitalized patients (Supplemental Figure 1B and Supplemental Figure 2). Only populations with at least 1 significant (adjusted *P* value < 0.05) difference between 2 groups were considered. We identified 13 immune subpopulations that were specifically increased or decreased in samples from SARS-CoV-2⁺ hospitalized patients compared with HCs and SARS-CoV-2⁻ hospitalized patients (Figure 3A, populations identified in green) and 16 subpopulations that were similarly altered in both groups of hospitalized patients compared with HCs (Figure 3A, populations identified in blue). The distribution of some of these subpopulations showing significant differences between our groups are illustrated (Figure 3, B and C). We observed alterations in the abundance of peripheral immune cell subpopulations (e.g., T cells, B cells, myeloid/monocytes, and neutrophils) compared with HCs in the acutely ill groups regardless of SARS-CoV-2 status; for example, a subset of CD19⁺ B cells (S2_Pop30; Figure 3B). In contrast, the abundance of specific immune cell subsets was elevated or reduced in SARS-CoV-2⁺ compared with SARS-CoV-2⁻ hospitalized patients; for example, a subset of CD27⁺CD8⁺ T cells (S3_Pop17; Figure 3C).

Table 3. Serological parameters in SARS-CoV-2⁺ patients

Serological parameter	Measure	Age		Statistics	COVID-19 severity		Statistics	Outcome at 30 days		Statistics	Mortality at 60 days, severe CoV-2⁺		Statistics
		<60 y.o.	≥60 y.o.	*P* value	Mild	Severe	*P* value	Good	Bad	*P* value	Survivor	Deceased	*P* value
Anti-S (FACS)	Median MFI (range)	12,672.5 (232–38,448)	3876 (232–48,281)	0.3059	4809 (232–38,448)	9702 (232–48,281)	0.6428	4844.5 (232–44,016)	6640.5 (232–48,281)	0.5013	7317.5 (232–48,281)	9702 (257–34,233)	0.6731
	Below positivity threshold	3/20	7/30		6/29	4/21		8/36	2/14		4/14	0/7	
IgM ELISA anti-RBD	Median (range)	18.90 (1.95–88.64)	3.51 (1.95–73.00)	0.04549	8.46 (1.95–61.70)	6.08 (1.95–88.64)	0.7866	9.13 (1.95–88.64)	4.07 (1.95–73.01)	0.5816	5.50 (1.95–88.64)	16.12 (1.95–73.005)	>0.9999
	Below positivity threshold	4/20	13/30		10/29	7/21		11/36	6/14		4/14	3/7	
IgG ELISA anti-RBD	Median (range)	44.85 (2.16–141.62)	24.42 (2.16–161.25)	0.3352	21.12 (2.16–141.62)	61.47 (2.16–161.25)	0.2688	24.42 (2.16–141.62)	55.22 (2.16–161.25)	0.3930	57.87 (2.16–147.51)	61.47 (2.16–161.25)	0.9596
	Below positivity threshold	4/20	11/30		9/29	6/21		11/36	4/14		4/14	2/7	
IgA ELISA anti-RBD	Median (range)	13.17 (0.76–113.57)	4.65 (0.76–100.21)	0.2530	6.22 (0.76–113.57)	10.71 (0.76–100.21)	0.6218	7.63 (0.76–113.57)	12.49 (0.76–100.21)	0.5222	8.31 (0.76–100.21)	18.05 (0.76–75.61)	0.7975
	Below positivity threshold	3/20	7/30		5/29	5/21		7/36	3/14		4/14	1/7	
Neutralization SARS-CoV-2 ID_{50}	Median (range)	279.32 (50–22,988.51)	154.05 (50–16,194.33	0.0967	187.62 (50–2600.78)	473.26 (50–22,988.51)	0.1742	190.67 (50–22,988.51)	363.63 (50–12,542.33)	0.6367	363.63 (50–22,988.51)	773.99 (50–12,542.33)	0.8530
	Below positivity threshold	3/20	13/30		9/29	7/21		11/36	5/14		5/14	2/7	

ID_{50}, inhibitory dilution to inhibit 50% of the infection. Statistical analysis by Mann–Whitney U test.

To corroborate and expand these observations, we used a hypothesis-driven approach based on conventional manual gating (Supplemental Figure 3). Figure 4 shows granulocyte, monocyte/antigen-presenting cell, and lymphocyte subsets with significant differences (adjusted *P* value < 0.05) according to status (HC or SARS-CoV-2⁻ or SARS-CoV-2⁺). In line with the results of the data-driven analysis, we found several immune cell populations that differed significantly from HCs in hospitalized patients but are associated with acute illness rather than being specific for COVID-19. Of note, the differences observed according to status (HC or SARS-CoV-2⁻ or SARS-CoV-2⁺) in general immune cell populations (e.g., lymphocytes) were consistent across the different panels (Figure 4). Importantly, we were able to identify significant and specific alterations in samples from SARS-CoV-2⁺ compared with HCs and SARS-CoV-2⁻ hospitalized patients; for example, upregulation of PD-1 on T cells (particularly $CD4^+$ T cells) (Figure 4, populations indicated by *).

Neutrophilia and lymphopenia predict outcomes but are associated with severity of illness and age rather than specific to SARS-CoV-2 infection. Previous studies have identified lymphopenia and neutrophilia as predictive of worse clinical outcomes in SARS-CoV-2 infection (8, 15, 16). Compared with HCs, we detected a significantly increased proportion of neutrophils and a corresponding decreased proportion of lymphocytes ($CD3^+$ T cells and $CD19^+$ B cells) in samples from hospitalized patients (Figures 4 and 5A). However, these changes were not specific to SARS-CoV-2 infection and were observed in both hospitalized groups. Because age represents an important factor shaping the immune system as well as one of the greatest risk factors for COVID-19 severity and mortality (2–6), we also compared these immune populations in HCs and younger patients (<60 years old), as well as in older patients (≥60 years old). We observed that lymphopenia and neutrophilia were most striking in older patients (Figure 5A) and in relation to the severity of the medical condition, independently of SARS-CoV-2 status or other acute illness status (Figure 5B). Of note, among younger patients, comparison of mild versus severe acute illness revealed similar trends in both groups for lymphopenia (mild vs. severe 43.30% ± 5.58% vs. 21.58% ± 17.63% SARS-CoV-2⁻; 33.13% ± 13.31% vs. 17.38% ± 9.56% SARS-CoV-2⁺) and neutrophilia (mild vs. severe 47.80% ± 6.07% vs. 67.85% ± 19.68% SARS-CoV-2⁻; 53.60% ± 10.32% vs. 69.29% ± 16.89% SARS-CoV-2⁺). Although not specific for SARS-CoV-2 infection, neutrophilia and lymphopenia, as well as a low proportion of $CD3^+$ but not $CD19^+$ cells, were in addition strongly tied to outcomes at 30 days (Figure 5C). Within the neutrophil compartment, we observed a statistically significant shift from $CD16^{hi}CD15^+$ to $CD16^{lo}CD15^+$ neutrophils in SARS-CoV-2⁺ and SARS-CoV-2⁻ patients compared with HCs (Figure 4 and 5A and Supplemental Figure 3), but no difference when

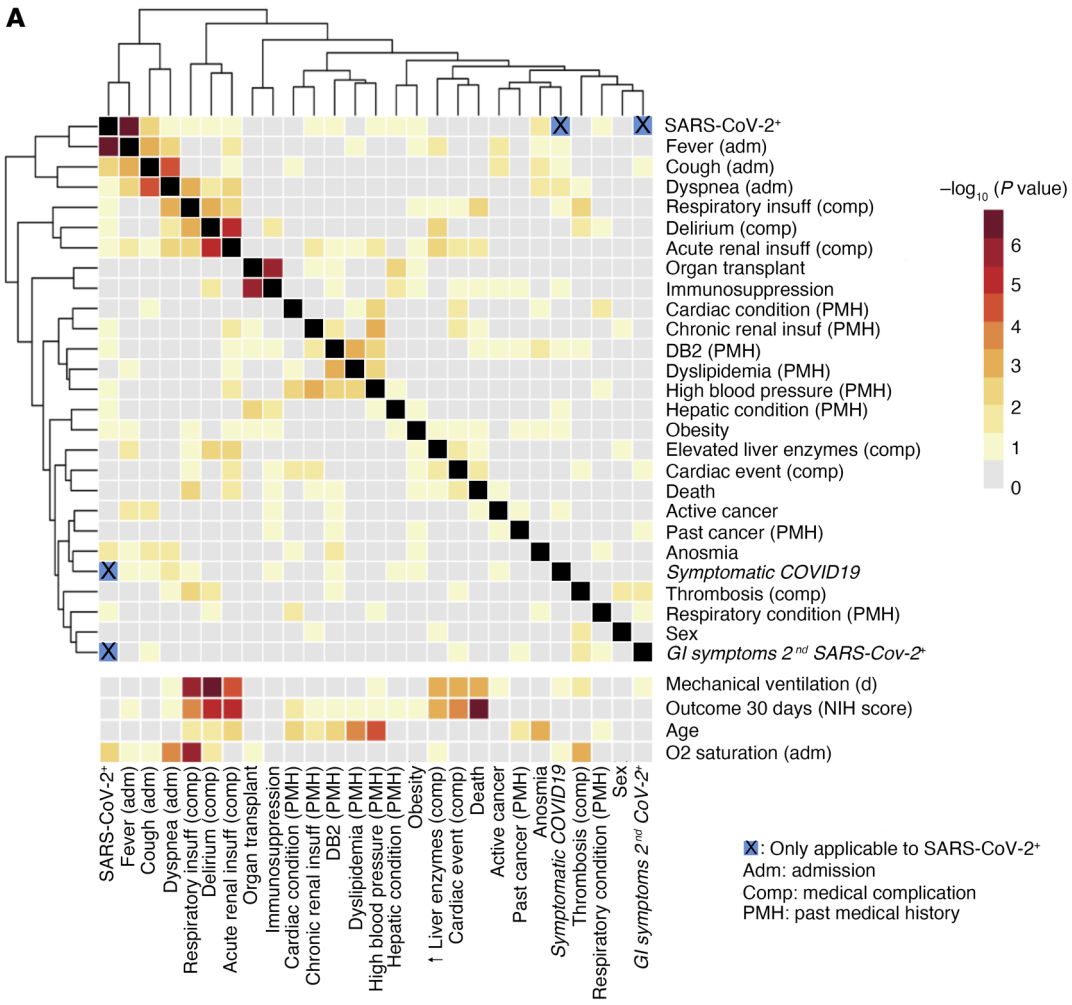

Figure 1. Clinical characteristics of hospitalized patients. Association among clinical parameters in hospitalized patients as illustrated by heatmap and hierarchical clustering of the $-\log_{10}$(*P* value). Fisher's exact test for association of binary variables (upper part), and Wilcoxon's rank-sum test for association between binary and continuous variables (lower part). Blue squares indicate that only SARS-CoV-2$^+$ patients were considered for this parameter.

comparing SARS-CoV-2$^+$ with SARS-CoV-2$^-$ patients and no association with disease severity (Figure 5B), which demonstrates that this shift was not specific to COVID-19. Within the CD3$^+$ T cell compartment, the CD4$^+$/CD8$^+$ ratio increased with older age as expected but was not different between groups of similar age, whereas CD3$^+$ γδT cells and invariant NK T (iNKT) cells were reduced in SARS-CoV-2$^+$ samples compared with HCs, but not different from SARS-CoV-2$^-$ samples in hospitalized patients nor associated with disease severity (Figure 5, A and B).

The frequency of NK cells was reduced in both groups of hospitalized patients compared with HCs (Figure 4), especially in individuals with a severe medical condition (COVID-19 or other acute illness) and was significantly lower in SARS-CoV-2$^+$ patients showing a worse clinical outcome at 30 days (Figure 5, A–C). Finally, as previously reported (23), we observed a decreased frequency of CD123$^+$ and CD11c$^+$ cells among the CD3$^-$CD19$^-$CD14$^-$CD56$^-$ cells (presumably DCs) in the peripheral blood of SARS-CoV-2$^+$ patients, but this was not significantly different from SARS-CoV-2$^-$ acutely ill patients. The frequency of monocytes was similar in HC, SARS-CoV-2$^-$, and SARS-CoV-2$^+$ patients (Figure 5A) but HLA-DR expression on CD14$^+$ monocytes was significantly reduced in both groups of hospitalized patients compared with HCs (Figure 4), indicating possible monocyte exhaustion, a phenomenon typically observed after acute intense monocyte inflammation as seen, for example, in sepsis (24). Altogether, our data confirmed previous reports linking neutrophilia and lymphopenia with severe COVID-19 and worse outcomes; however, we demonstrated that these changes were associated with age and severity of the medical condition rather than being specific for SARS-CoV-2 infection.

SARS-CoV-2 infection is associated with a significantly higher proportion of circulating promyelocytes and mature neutrophils but not activated neutrophils. Because significant neutrophilia was observed in SARS-CoV-2$^-$ and SARS-CoV-2$^+$ patients compared with HCs (Figure 4), we investigated whether neutrophil subsets within the granulocytes' gate (CD14$^-$ cells in the neutrophil FSC-SSC gate) were specifically altered in SARS-CoV-2$^+$ patients and associated with severity. The proportion of promyelocytes (CD38$^+$), precursors of granulocytes, was significantly higher in SARS-CoV-2$^+$ patients compared with SARS-CoV-2$^-$ patients and HCs (Figure 4); this increased percentage of pro-

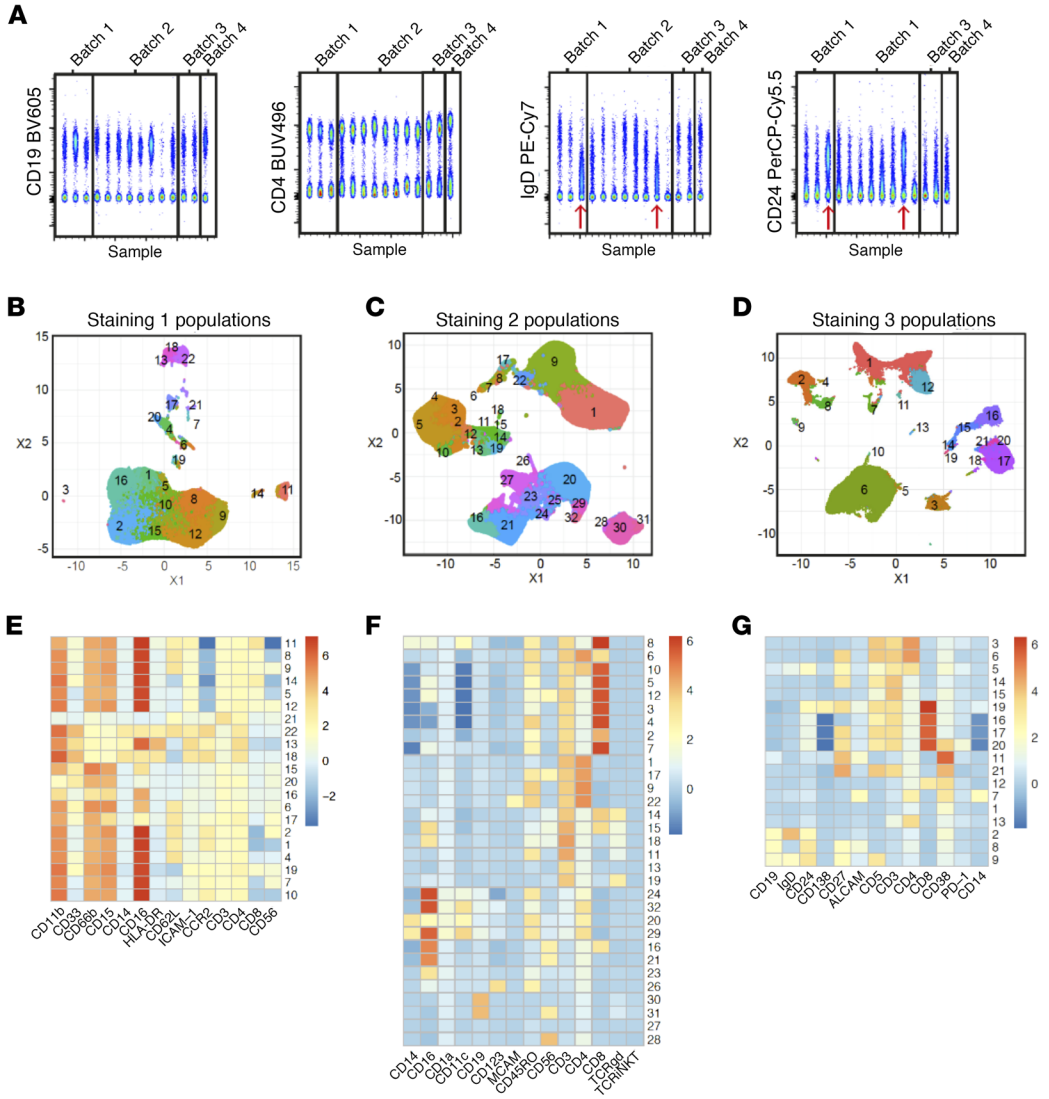

Figure 2. Data-driven flow cytometry analysis. (**A**) Representative dot plots of multiple samples acquired in 4 different batches for CD19-BV605, CD4-BUV496, IgD-PE-Cy7, and CD24-PerCP-Cy5.5. Red arrows identify samples from the same individual acquired in 2 different batches. (**B**–**D**) Representation of FlowSOM populations on UMAP projection axis and (**E**–**G**) their corresponding heatmaps showing geometric mean fluorescence of the different markers for the different subpopulations (data-driven analysis). Cellular markers are indicated on the *x* axis and population number on the *y* axis of heatmaps.

myelocytes was, however, not significantly different according to severity, and did not lead to differing outcomes at 30 days (Figure 6, A–C). In parallel, the frequency of mature neutrophils ($CD16^{hi}CD15^{+}CD11b^{hi}CD62L^{hi}$) was specifically increased in the peripheral blood in SARS-CoV-2^{+} patients (Figure 4), whereas that of activated neutrophils ($CD16^{hi}CD15^{+}CD11b^{hi}CD62L^{lo}$) was lower, but these subsets were not associated with severe COVID-19 (Figure 6B and Supplemental Figure 3B). Our results suggest that specific stages of neutrophils were overrepresented in the peripheral blood of SARS-CoV-2^{+} patients, while most circulating activated neutrophils that might have already infiltrated organs (e.g., lungs) died of overstimulation (NETosis) after acute infection and/or were immunosuppressed, as previously reported (25).

Expression of MHC-related molecule CD1a on monocytes is associated with SARS-CoV-2 status, severity, and outcomes. We also assessed whether specific subpopulations of antigen-presenting cells were altered in SARS-CoV-2^{+} patients and associated with severity because these could secrete multiple inflammatory mediators (cytokines, myeloperoxidases, ROS, etc.) and present antigen to T cells. Within the monocyte compartment, monocytes bearing CD16 (FCγIIIR) are associated with antigen-presentation, tissue homing, and secretion of proinflammatory cytokine TNF (26). The proportion of classical $CD14^{hi}CD16^{-}$ monocytes was specifically reduced in SARS-CoV-2^{+} patients compared with HCs and SARS-CoV-2^{-} patients; in contrast, the frequency of intermediate $CD14^{hi}CD16^{+}$ monocytes was specifically augmented in SARS-CoV-2^{+} patients (Figures 4 and 6A) but was not significantly associated with severity (Supplemental Figure 3B) or outcome (data not shown). Notably, the proportion of $CD14^{+}$ monocytes expressing CD1a, which is implicated in lipid-antigen presentation to T cells and is induced on $CD14^{+}$ monocytes exposed to IL-4 and GM-CSF (27), was also increased in SARS-CoV-2^{+} patients compared with HCs and SARS-CoV-2^{-} patients regardless of age (Figures 4 and 6A). Moreover, $CD1a^{+}CD14^{+}$ monocytes were more prevalent in SARS-CoV-2^{+} patients exhibiting severe symptoms and in SARS-CoV-2^{+} patients experiencing an unfavorable outcome at 30 days. Overall, our results suggest that in response to SARS-CoV-2 infection, specific subsets of peripheral blood antigen-presenting cells are altered.

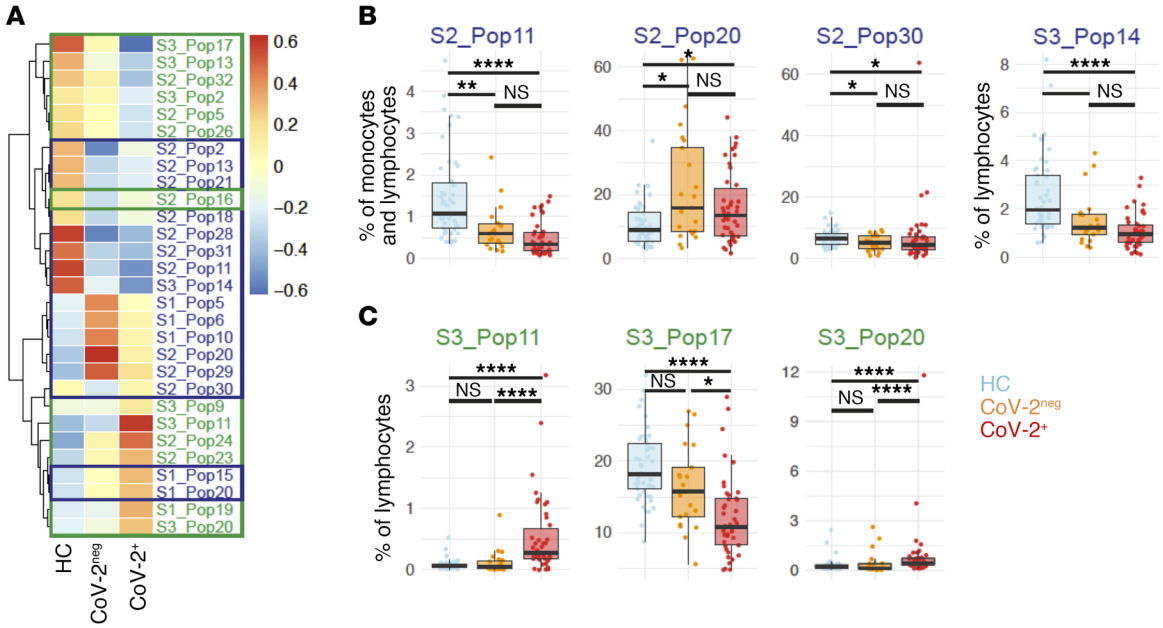

Figure 3. Data-driven analysis shows common and distinct alterations in immune cell populations in SARS-CoV-2$^+$ and SARS-CoV-2$^-$ hospitalized patients. (**A**–**C**) Data-driven analysis. (**A**) Heatmap showing the median frequencies of immune cell populations differentially regulated in SARS-CoV-2$^+$ patients (CoV-2$^+$), SARS-CoV-2$^-$ patients (CoV-2$^-$), and healthy control (HC) samples. (**B** and **C**) Box-and-whisker plots showing frequencies of dysregulated immune cell populations in (**B**) CoV-2$^+$ (red) compared with CoV-2$^-$ (yellow) and HC (blue) and in (**C**) hospitalized patients (both CoV-2$^+$ and CoV-2$^-$) compared with HC (blue). HC, n = 49; CoV-2$^-$, n = 21; CoV-2$^+$, n = 42. Kruskal-Wallis test followed by a Dunn's post hoc test for multiple pairwise comparisons. *P < 0.05; **P < 0.01; ****P < 0.0001.

B cell subsets are altered in SARS-CoV-2 infection. B cell–depleting therapies are associated with a higher risk of severe COVID-19 course (28), and several publications support the contribution of NAbs to the immune response in SARS-CoV-2 infection (29–32). Because we detected a reduction in peripheral blood B cells in hospitalized patients compared with HCs, we further assessed the frequency of specific B cell subpopulations in our cohort and association with severity using CD5, CD27, and IgD as subset markers. We found that the proportion of B cells expressing CD5 was significantly reduced in SARS-CoV-2$^-$ and SARS-CoV-2$^+$ patients compared with HCs (Figure 4), but this reduction was more pronounced in SARS-CoV-2$^+$ patients, especially in patients experiencing a severe clinical course or showing an unfavorable clinical outcome at 30 days (Figure 6, A–C). Notably, CD5$^+$ B cells play a crucial role in innate immunity (33) and include natural polyreactive antibody–producing cells (34) and IL-10–producing regulatory cells (35). Analysis of B cells according to their expression of IgD and CD27 revealed a significantly higher proportion of IgD$^-$CD27$^-$ B cells in SARS-CoV-2$^+$ patients compared with HCs and SARS-CoV-2$^-$ patients (Figure 4); this increase was more pronounced in older patients (Figure 6A) but did not differ according to severity (Supplemental Figure 3B) or outcome (data not shown). This IgD$^-$CD27$^-$ B cell subset is expanded in the peripheral blood of patients with inflammatory diseases or viral infections and upon aging (36–39). In contrast, the other subpopulations (CD27$^+$IgD$^-$, CD27$^+$IgD$^+$, CD27$^-$IgD$^+$) were either similarly prevalent in all 3 groups or comparable between SARS-CoV-2$^-$ and SARS-CoV-2$^+$ patients (Figure 4 and Supplemental Figure 3A). Further classification of subsets of naive, unswitched memory, switched memory, and double-negative B cells according to CD24 and CD38 expression did not reveal expression patterns specific to SARS-CoV-2 infection except for a reduction in the abundance of preswitched/resting memory B cells (CD27$^+$IgD$^-$CD24$^+$CD38$^{+/lo}$), which was more pronounced in older SARS-CoV-2$^+$ patients (Figure 4 and Supplemental Figure 3A) but not associated with disease severity (P = 0.41) or outcome (P = 0.45). Overall, our results demonstrated alterations of specific B cell subpopulations (reduced CD5$^+$ and increased IgD$^-$CD27$^-$) in SARS-CoV-2$^+$ patients compared with the other groups, suggesting a shift toward a proinflammatory B cell profile.

Activated CD38$^+$CD8$^+$ T cells and PD-1$^+$CD4$^+$ T cells characterize SARS-CoV-2$^+$ patients and are associated with outcome. We investigated whether multiple markers (PD-1, CD38, CD27, CD56), triggered on activated or memory T cell subpopulations and associated with antiviral responses, are altered in SARS-CoV-2$^+$ patients and associated with severity. CD38 has been linked to T cell functions, such as protection from cell death (40) and high suppressive activity by regulatory T cells, and to disease progression in HIV patients (40). We found that CD38 expression was strongly upregulated on CD8$^+$ T cells in SARS-CoV-2$^+$ patients compared with SARS-CoV-2$^-$ patients and HCs (Figure 4) regardless of age (Figure 6A). Levels tended to be higher in severe COVID-19 compared with mild/moderate SARS-CoV-2 infection (Figure 6B). Importantly, the percentage of CD38$^+$CD8$^+$ T cells was significantly higher in the worse outcome group at 30 days (Figure 6C). Our results suggest that an elevated frequency of CD38$^+$CD8$^+$ T cells represents a biomarker for a protracted course of severe COVID-19 still requiring supplemental oxygenation at 30 days. We observed a significant reduction in the proportion of CD4$^+$ T cells expressing CD38 in SARS-CoV-2$^-$ and SARS-CoV-2$^+$ patients

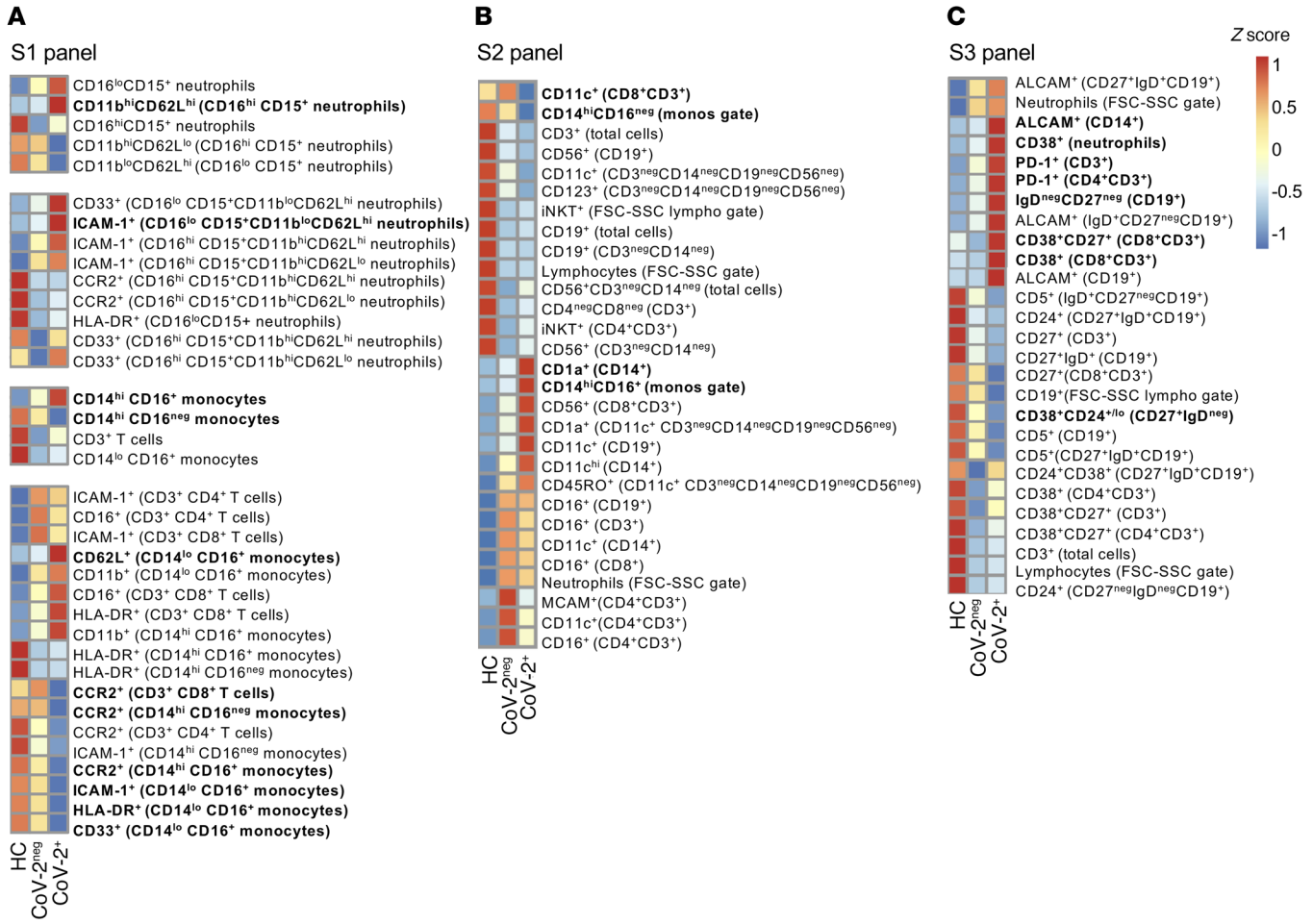

Figure 4. Hypothesis-driven analysis identifies common and distinct alterations in immune cell populations in SARS-CoV-2$^+$ and SARS-CoV-2$^-$ hospitalized patients. (**A**–**C**) Hypothesis-driven (based on conventional manual gating) analysis. Heatmaps showing the median frequency of immune cell populations identified as significantly altered (adjusted $P < 0.05$) in CoV-2$^+$ ($n = 50$) compared with HC ($n = 49$) and/or CoV-2$^-$ ($n = 22$) in stain 1 (S1 panel), stain 2 (S2 panel), and stain 3 (S3 panel). Kruskal-Wallis test followed by a Dunn's post hoc test for multiple pairwise comparisons. Nominal P values were adjusted for multiple testing within each stain, FDR significance threshold set at 0.05. Color scale indicates the z score, across the groups, of subpopulation median frequencies. *$P < 0.05$ for populations significantly altered in SARS-CoV-2$^+$ compared with HC and with SARS-CoV-2$^-$ samples. Monos, monocytes; Neutros, neutrophils; Lymphos, lymphocytes.

compared with HCs (Figure 4) without any significant association with age, severity, or outcome (Supplemental Figure 3).

PD-1 is an immune checkpoint molecule associated with T cell activation and exhaustion (41). The proportion of PD-1–expressing CD3$^+$ T cells and more specifically CD4$^+$ T cells was elevated in older and younger SARS-CoV-2$^+$ patients compared with SARS-CoV-2$^-$ hospitalized patients and HCs (Figures 4 and 6A). PD-1 expression was not associated with disease severity among SARS-CoV-2$^+$ samples (Figure 6B), but the percentage of PD-1$^+$CD4$^+$ T cells was significantly higher in SARS-CoV-2$^+$ patients who had an unfavorable outcome at 30 days (Figure 6C). Expression of PD-1 on CD8$^+$ T cells was higher in SARS-CoV-2$^+$ patients compared with HCs, but this was almost exclusively observed in older patients and did not significantly differ from SARS-CoV-2$^-$ hospitalized patients (Supplemental Figure 3A). Finally, the percentages of CD8$^+$ T cells expressing CD27 and CD56 were respectively reduced and increased compared with HCs and showed a similar trend compared with SARS-CoV-2$^-$ patients but were not associated with severity (Figure 4 and Supplemental Figure 3, A and B). Overall, our results showed that CD38 on CD8$^+$ T cells and PD-1 on CD4$^+$ T cells were specifically altered in SARS-CoV-2$^+$ patients and associated with outcome at 30 days.

Upregulation of specific trafficking molecules distinguishes SARS-CoV-2 infection, COVID-19 severity, and clinical outcomes. Diapedesis of circulating leukocytes is a crucial inflammatory step in immune responses that, when out of control, can cause serious collateral damage (42, 43). To determine whether COVID-19 affects the trafficking potential of circulating leukocytes, we assessed a selection of key trafficking molecules (ICAM-1, ALCAM, CCR2, CD11c) on the different immune subsets. In granulocytes, we observed that the proportion of mature and activated neutrophils expressing ICAM-1 (44) was increased in hospitalized patients compared with HCs and more so in SARS-CoV-2$^+$ patients (Figures 4 and 6A and Supplemental Figure 3), especially those exhibiting severe disease and experiencing an unfavorable outcome at 30 days (Figure 6, B and C). These data suggest that ICAM-1$^+$ neutrophils, which have been

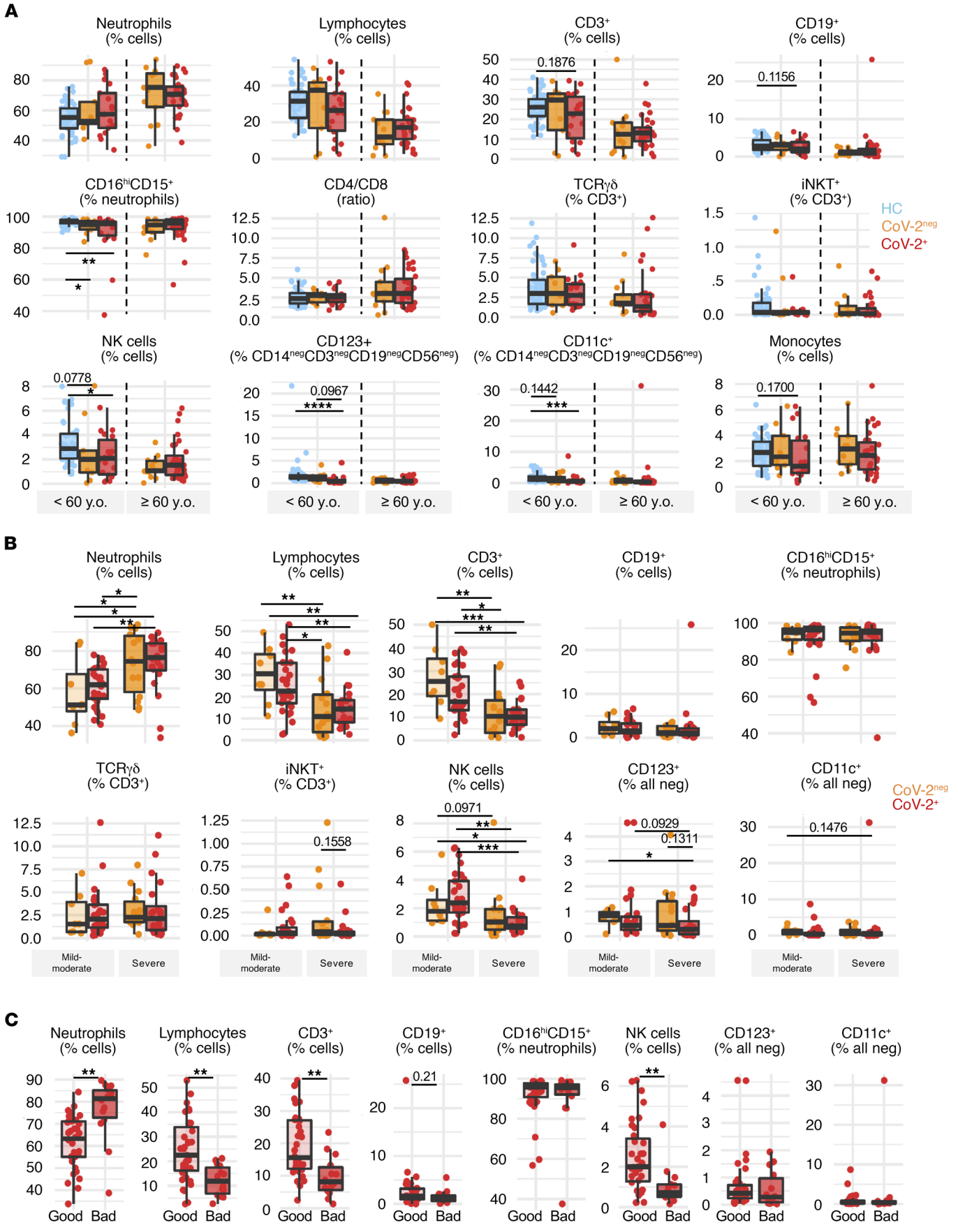
A
Neutrophils (% cells)
Lymphocytes (% cells)
CD3+ (% cells)
0.1876
CD19+ (% cells)
0.1156
CD16hiCD15+ (% neutrophils)
CD4/CD8 (ratio)
TCRγδ (% CD3+)
iNKT+ (% CD3+)
HC
CoV-2neg
CoV-2+
NK cells (% cells)
0.0778
CD123+ (% CD14negCD3negCD19negCD56neg)
0.0967
CD11c+ (% CD14negCD3negCD19negCD56neg)
0.1442
Monocytes (% cells)
0.1700
< 60 y.o.
≥ 60 y.o.
B
Neutrophils (% cells)
Lymphocytes (% cells)
CD3+ (% cells)
CD19+ (% cells)
CD16hiCD15+ (% neutrophils)
TCRγδ (% CD3+)
iNKT+ (% CD3+)
0.1558
NK cells (% cells)
0.0971
CD123+ (% all neg)
0.0929
0.1311
CD11c+ (% all neg)
0.1476
CoV-2neg
CoV-2+
Mild-moderate
Severe
C
Neutrophils (% cells)
Lymphocytes (% cells)
CD3+ (% cells)
CD19+ (% cells)
0.21
CD16hiCD15+ (% neutrophils)
NK cells (% cells)
CD123+ (% all neg)
CD11c+ (% all neg)
Good
Bad

Figure 5. Alterations in immune cell populations commonly observed in SARS-CoV-2$^+$ and SARS-CoV-2$^-$ hospitalized patients. (**A**–**C**) Frequencies of different subsets of immune cell populations in peripheral blood (hypothesis-driven analysis based on conventional manual gating) from SARS-CoV-2$^+$ (CoV-2$^+$, red) and SARS-CoV-2$^-$ (CoV-2$^-$, yellow) hospitalized patients and healthy controls (HC, blue) (**A**) according to age group (HC <60 years n = 49; CoV-2$^-$ hospitalized <60 years n = 9, ≥60 years n = 13; CoV-2$^+$ <60 years n = 20, ≥60 years n = 30), (**B**) according to disease severity in hospitalized patients (CoV-2$^-$ mild/moderate disease n = 8, severe disease n = 14; CoV-2$^+$ mild/moderate disease n = 29, severe disease n = 21), and (**C**) according to clinical outcome at 30 days in SARS-CoV-2$^+$ patients (NIH score 5–8, n = 36) versus (NIH score 1–4, n = 14). Mann-Whitney U test (for n = 2 categories) and Kruskal-Wallis test (for n > 2 categories) followed by Dunn's post hoc test for multiple pairwise comparisons were used. Each symbol represents 1 donor. *P < 0.05; **P < 0.01; ***P < 0.001; ****P < 0.0001.

associated with dissemination of inflammation through reverse transendothelial migration, cellular aggregation, and effector function (45–47), could participate to fuel the proinflammatory cascade observed in COVID-19.

Strikingly, the percentage of monocytes (CD14$^+$) expressing the cell adhesion molecule ALCAM was strongly upregulated in SARS-CoV-2$^+$ patients compared with HCs and SARS-CoV-2$^-$ patients (Figures 4 and 6A). This increased frequency was found in younger and older patients and was significantly higher in patients with severe COVID-19 and elevated in patients who showed an unfavorable outcome at 30 days (Figure 6, B and C). ALCAM is associated with leukocyte transendothelial migration and with the stabilization of the immune synapse (48, 49). This suggests that monocytes from SARS-CoV-2$^+$ patients could be poised to activate lymphocytes and interact with the endothelium, thus participating in general inflammatory processes.

Inversely, CCR2, a chemokine receptor implicated in recruitment of monocytes to pulmonary alveolar tissue (50), was expressed by a reduced percentage of monocytes (CD14$^+$) in SARS-CoV-2$^+$ patients compared with SARS-CoV-2$^-$ patients (Figures 4 and 6A). This reduction was not associated with disease severity but was significantly more pronounced in SARS-CoV-2$^+$ patients with an unfavorable outcome at 30 days (Figure 6, B and C). Because the bronchoalveolar fluid from COVID-19 patients has been shown to contain abundant inflammatory monocyte-derived macrophages and CCR2 ligand CCL2 (51), the reduced proportion of CCR2$^+$ monocytes in the periphery could result from preferential transmigration of these subsets in the inflamed lungs or simply reflect the reduction in classical monocytes, which also express CCR2.

Among T cells, CCR2 expression was also reduced in SARS-CoV-2$^+$ patients (Figure 4) but did not significantly correlate with severity or outcome (good vs. bad outcome: CD4$^+$CCR2$^+$ 14.42% ± 1.11% vs. 11.80% ± 1.72%, P = 0.24; CD8$^+$CCR2$^+$ 8.53% ± 1.07% vs. 7.09% ± 1.32%, P = 0.71). The frequency of CD8$^+$ T cells bearing CD11c β2 integrin was significantly lower in the blood of SARS-CoV-2$^+$ compared with SARS-CoV-2$^-$ patients (Figures 4 and 6A), especially in severe cases (Supplemental Figure 3B), but did not correlate with outcome among SARS-CoV-2$^+$ patients (P = 0.33). Notably, this T cell subset has antiviral properties and can accumulate in the lungs during infection (52) and can suppress pathogenic T cells in autoimmunity (53). The proportion of B cells expressing CD11c or ALCAM followed a similar pattern (Figure 4), with a specific upregulation of both markers on B cells from SARS-CoV-2$^+$, especially in patients over 60 years old compared with HCs and SARS-CoV-2$^-$ patients; however, there was no significant difference between mild/moderate and severe COVID-19 symptoms (Supplemental Figure 3B) or according to outcome among SARS-CoV-2$^+$ patients.

Multivariate analysis confirms independent associations of identified immune cell populations with SARS-CoV-2 status. Using random forest class prediction analysis (54), we explored whether the immune cell populations identified by the univariate nonparametric Kruskal-Wallis tests as associated with SARS-CoV-2 status are also independently associated with status in a multivariate model. We confirmed that frequencies of ICAM-1$^+$ activated neutrophils; CCR2$^+$, CD1a$^+$, and ALCAM$^+$ monocytes; CD38$^+$CD8$^+$ T cells; and PD-1$^+$CD4$^+$ T cells were all among the top 30 important predictive features, as measured by the Gini importance index (Supplemental Figure 4 and ref. 54), to discern between HCs and hospitalized patients. However, CD5$^+$ B cells were not found to be of high importance in distinguishing between HCs and SARS-CoV-2$^+$ patients in this multivariate analysis. Of note, HCs and SARS-CoV-2$^+$ patients but not SARS-CoV-2$^-$ patients were classified with a high accuracy. Such inaccuracy to classify SARS-CoV-2$^-$ patients is probably due to the lower number of patients and the greater heterogeneity of diseases in this group.

Finally, because we could not directly assess the impact of normal aging on the immune profile in a group of HCs over 60 years old, we assessed whether age could represent a confounding factor for the association between the immune cell populations identified and SARS-CoV-2 versus HC status. Using linear regression models with and without adjusting for age in all individuals under 60 years old, we found no large confounding bias of age on the association. In line with this, we found no significant correlation of age with identified immune cell populations in HCs, except for a small decrease in the frequency of CD38$^+$CD8$^+$ T cells, IgD$^-$CD27$^-$ B cells, and CD1a$^+$ monocytes (Supplemental Figure 6).

COVID-19 mortality is associated with higher frequencies of ICAM-1$^+$ neutrophils, ALCAM$^+$ monocytes, and CD38$^+$CD8$^+$ T cells. We next determined whether the immune subpopulations we identified as dysregulated in hospitalized patients (24 populations) are associated with selected clinical parameters (Figure 7A). Sex, obesity, and days since onset of symptoms did not show strong correlations with most immune parameters. Although not specific to SARS-CoV-2$^+$ patients, neutrophilia and lymphopenia, especially low CD3$^+$ T cell count, were associated with medical complications, invasive ventilation, and mortality in SARS-CoV-2$^+$ patients. In addition, we found that most immune subpopulations specifically altered in SARS-CoV-2$^+$ patients and linked with severity and outcome were similarly associated with medical complications, invasive ventilation, and mortality (Figures 7A and 8). When looking specifically among severe COVID-19 patients requiring invasive ventilation, those who did not survive at 60 days had a significantly higher proportion of ICAM-1$^+$ cells among activated and mature neutrophils (Figure 7B). In addition, deceased patients showed a higher proportion of monocytes expressing ALCAM$^+$ but a trend toward a reduced proportion expressing CCR2. Finally, a higher

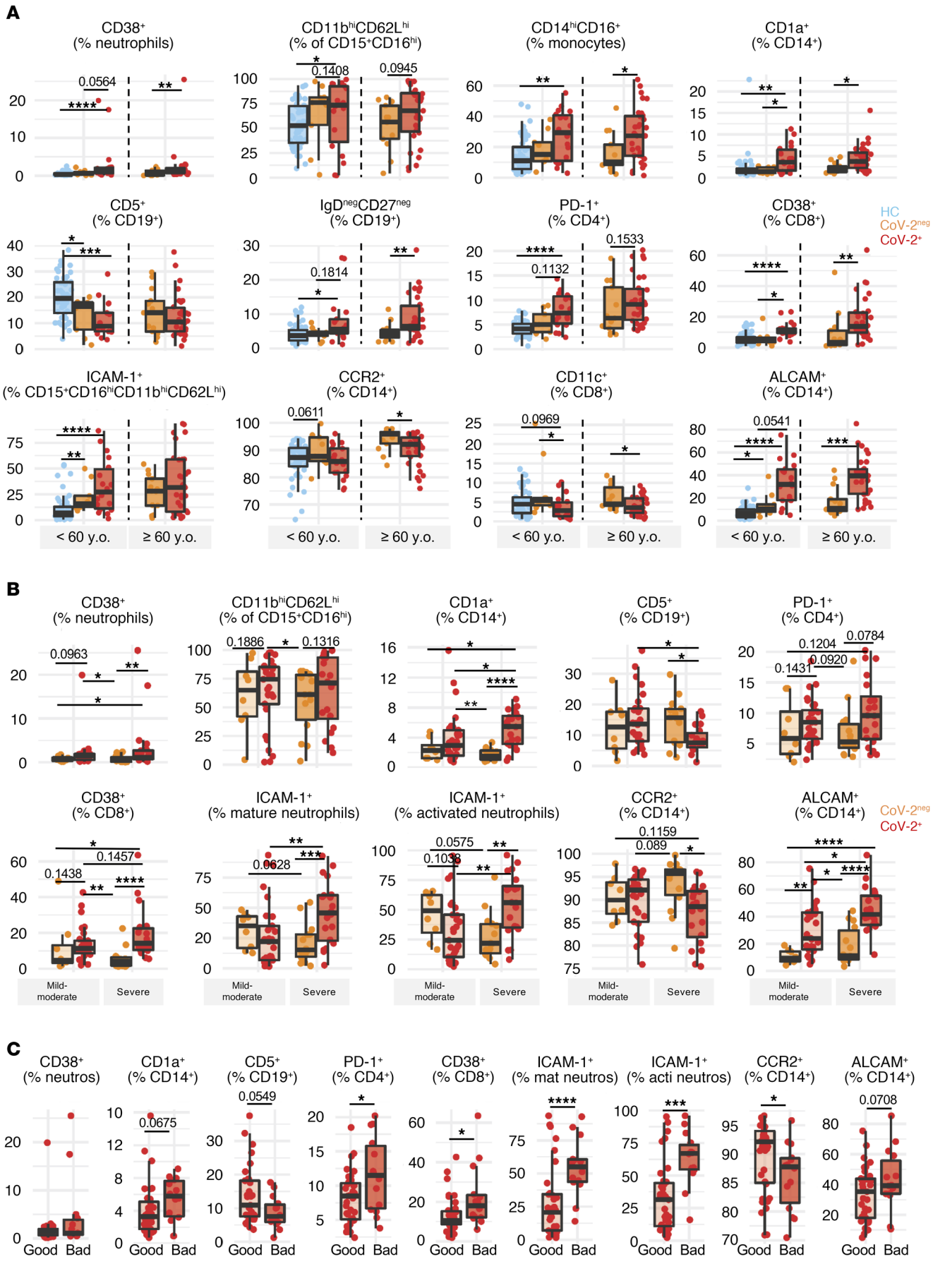
A
CD38+ (% neutrophils)
CD11bhiCD62Lhi (% of CD15+CD16hi)
CD14hiCD16+ (% monocytes)
CD1a+ (% CD14+)
CD5+ (% CD19+)
IgDnegCD27neg (% CD19+)
PD-1+ (% CD4+)
CD38+ (% CD8+)
HC
CoV-2neg
CoV-2+
ICAM-1+ (% CD15+CD16hiCD11bhiCD62Lhi)
CCR2+ (% CD14+)
CD11c+ (% CD8+)
ALCAM+ (% CD14+)
< 60 y.o.
≥ 60 y.o.
B
CD38+ (% neutrophils)
CD11bhiCD62Lhi (% of CD15+CD16hi)
CD1a+ (% CD14+)
CD5+ (% CD19+)
PD-1+ (% CD4+)
CD38+ (% CD8+)
ICAM-1+ (% mature neutrophils)
ICAM-1+ (% activated neutrophils)
CCR2+ (% CD14+)
ALCAM+ (% CD14+)
CoV-2neg
CoV-2+
Mild-moderate
Severe
C
CD38+ (% neutros)
CD1a+ (% CD14+)
CD5+ (% CD19+)
PD-1+ (% CD4+)
CD38+ (% CD8+)
ICAM-1+ (% mat neutros)
ICAM-1+ (% acti neutros)
CCR2+ (% CD14+)
ALCAM+ (% CD14+)
Good
Bad

Figure 6. Alterations in immune cell populations distinguishing SARS-CoV-2$^+$ from SARS-CoV-2$^-$ hospitalized patients. (**A**–**C**) Frequencies of different subsets of immune cell populations in peripheral blood (hypothesis-driven analysis based on conventional manual gating) from SARS-CoV-2$^+$ (CoV-2$^+$, red) and SARS-CoV-2$^-$ (CoV-2$^-$, yellow) hospitalized patients and healthy controls (HC, blue) (**A**) according to age groups (HC <60 years n = 49; CoV-2$^-$ hospitalized <60 years n = 9, ≥60 years n = 13; CoV-2$^+$ <60 years n = 20, ≥60 years n = 30), (**B**) according to disease severity in hospitalized patients (CoV-2$^-$ mild/moderate disease n = 8, severe disease n = 14; CoV-2$^+$ mild/moderate disease n = 29, severe disease n = 21), and (**C**) according to clinical outcome at 30 days in SARS-CoV-2$^+$ patients (NIH score 5–8, n = 36) versus (NIH score 1–4, n = 14). Mann-Whitney U test (for n = 2 categories) and Kruskal-Wallis test (for n > 2 categories) followed by Dunn's post hoc test for multiple pairwise comparisons were used. Each symbol represents 1 donor. *P < 0.05; **P < 0.01; ***P < 0.001; ****P < 0.0001.

proportion of CD38$^+$CD8$^+$ T cells (Figure 7, A and B) was observed in deceased severe COVID-19 patients compared with survivors. The other SARS-CoV-2$^+$–specific dysregulated immune populations (PD-1$^+$CD4$^+$ T cells, CD5$^+$ B cells, CD1a$^+$ monocytes) were not significantly altered in deceased individuals with severe COVID-19 compared with survivors with severe COVID-19 (Figure 8).

Longitudinal analysis reveals increasing expression of CD38 and PD-1 on T cells in patients with unfavorable outcome. We were able to obtain follow-up samples at 24–72 hours (t1) and at 4–8 days (t2) after baseline sample collection (t0) in a subset of SARS-CoV-2$^+$ patients. Using a semiparametric approach, generalized estimation equations (55), we examined the trend over time in selected populations identified as specific to COVID-19. We did not observe a significant trend for ICAM-1$^+$ neutrophils or CD1a$^+$ or CCR2$^+$ monocytes but found the expression of ALCAM on monocytes to be consistently and significantly lower over time in SARS-CoV-2$^+$ patients showing a favorable outcome, but not in those showing an unfavorable outcome, at 30 days (Figure 7C). On the contrary, although the patients with a good outcome at 30 days did not show a significant change in the proportion of their B cells expressing CD5 over time, patients with a bad outcome almost all presented an increase at follow-up, starting from lower levels at first sampling. The proportion of CD38$^+$CD8$^+$ T cells doubled over time in patients with COVID-19 regardless of outcome; therefore, the increased frequency in patients with a bad outcome remained present at follow-up. Finally, although levels were not significantly different over time in SARS-CoV-2$^+$ patients displaying a favorable outcome at 30 days, expression of PD-1 on CD4$^+$ T cells significantly increased over time in most patients experiencing a bad outcome at 30 days and were strongly upregulated at follow-up in 3/4 of patients who did not survive.

Discussion

Understanding the specific immune responses associated with SARS-CoV-2 infection is paramount to the quest for targeted therapy. Many groups have reported immune dysregulations in circulating leukocytes from patients infected with SARS-CoV-2 compared with healthy, often younger, individuals (14–16, 56, 57). Most of them, however, did not investigate whether these changes were specific to SARS-CoV-2 infection or represent nonspecific remodeling of the immune system in response to stress inherent to acute illness. Indeed, other critical noninfectious medical conditions are associated with immune perturbations (58). To discriminate the specific impact of SARS-CoV-2 infection on the immune system, we took a broader approach and included hospitalized SARS-CoV-2$^-$ patients who were acutely ill and comparable to SARS-CoV-2$^+$ patients in regards to age and sex, and we performed a whole blood flow cytometry analysis. We found multiple immune dysregulations in hospitalized patients compared with healthy participants (Figures 3 and 4). Nevertheless, we established specific differences in myeloid (e.g., elevated proportion of ALCAM$^+$ monocytes) and lymphocyte (e.g., increased percentage of CD38$^+$CD8$^+$ T cells) subpopulations in SARS-CoV-2$^+$ compared with SARS-CoV-2$^-$ patients (Figure 6A). Finally, a subset of these immune alterations correlated with disease severity and outcome (Figures 5, B and C; 6, B and C; 7, A and B; and 8). Overall, our study provides the groundwork to develop specific peripheral blood biomarkers to stratify SARS-CoV-2$^+$ patients at risk of unfavorable outcomes and identify candidate molecules as potential therapeutic targets.

We observed changes in the proportions of key white blood cell subsets: neutrophils and lymphocytes. Indeed, we did detect lymphopenia and neutrophilia in hospitalized patients regardless of their SARS-CoV-2 status; the most severe perturbations were found in older patients and were associated with disease severity as well as disease outcome (Figure 5). Although other groups have linked severe SARS-CoV-2 infection with lymphopenia (59), our results as well as those from others (60) support the notion that lymphopenia is in fact commonly observed in critically ill patients, especially in older patients, although also present in younger individuals, and not related to the SARS-CoV-2 infection (58, 61). Nevertheless, we found alterations in both innate and adaptive immune cell subpopulations that were specifically associated with SARS-CoV-2 infection.

We observed elevated proportions of proinflammatory innate immune cell subsets. Notably, the frequency of CD38$^+$ neutrophils was increased in SARS-CoV-2$^+$ patients (Figure 6). CD38 expression during neutrophil activation has been shown to play an essential role for appropriate control of pathogen infection and cell migration in affected organs (40). SARS-CoV-2$^+$ patients had a higher proportion of CD14^{hi}CD16$^+$ monocytes than SARS-CoV-2$^-$ patients. This monocyte subset shows robust ROS and TNF production and strongly promotes proliferation and antigen presentation to T cells (26). In addition, the frequency of CD1a$^+$CD14$^+$ monocytes was higher in SARS-CoV-2$^+$ compared with SARS-CoV-2$^-$ patients, and such alteration was associated with worse clinical outcomes (Figure 6C). CD1a$^+$CD14$^+$ monocytes can activate and induce differentiation of proinflammatory IFN-γ$^+$CD4$^+$ T cells (62). We found a depletion of CD5$^+$ B cells, which comprise B-1a cells and play a crucial role in innate immunity, in our 2 groups of hospitalized patients, although this depletion was more pronounced in SARS-CoV-2$^+$ patients and most striking in SARS-CoV-2$^+$ patients with an unfavorable outcome (Figure 6C). Such depletion has been described in sepsis (63) and SARS-CoV-2 infection (57, 64). CD5$^+$ B cells can secrete inhibitory cytokines (65) and natural IgM as an early response to pathogen invasion and promote tissue homeostasis and facilitate clearance of apoptotic cells (33). B-1a cells regulate neutrophil lung infiltration, inhibit the production of myeloperoxidase, and modulate mac-

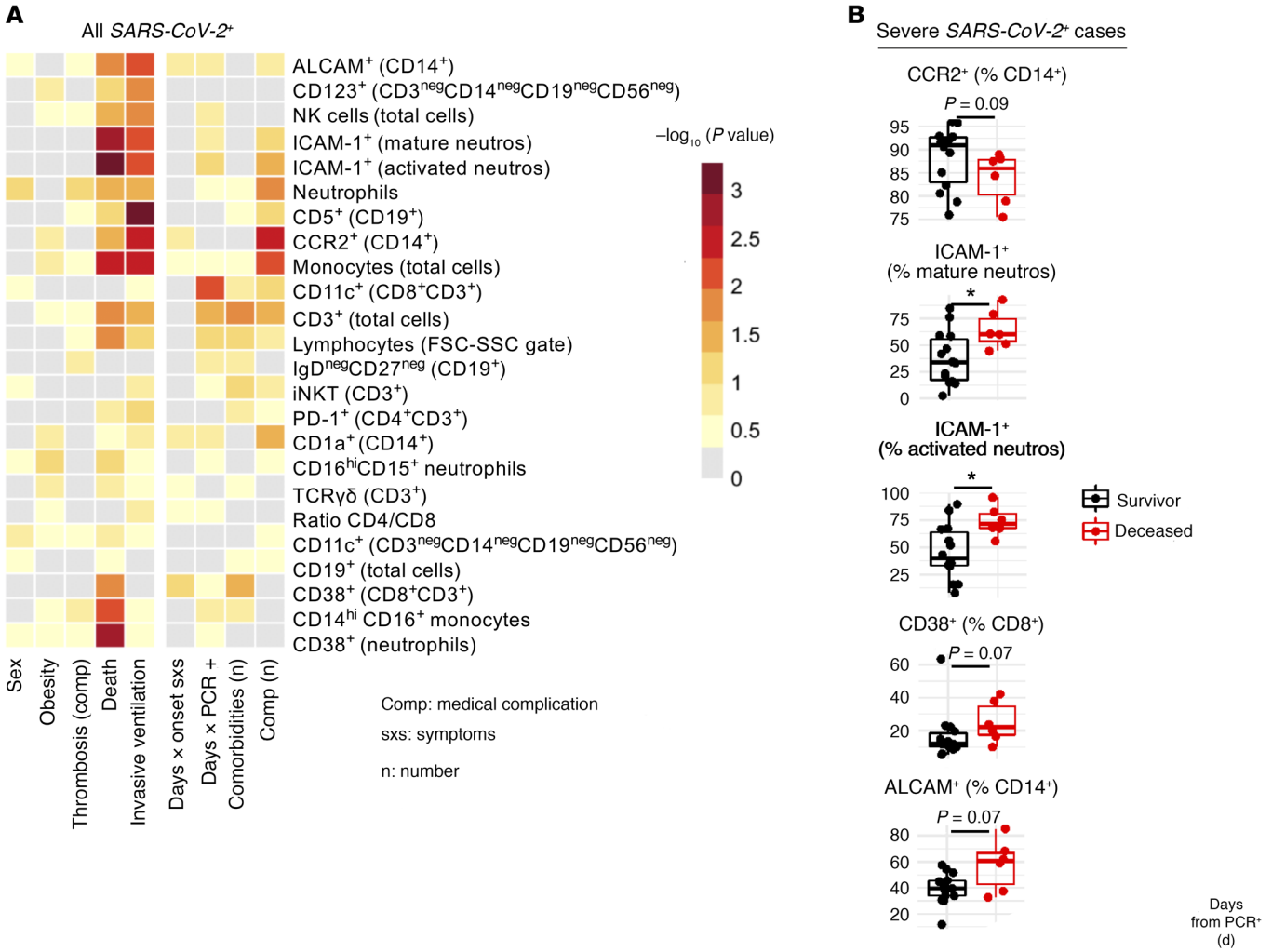
A
All SARS-CoV-2+
ALCAM+ (CD14+)
CD123+ (CD3negCD14negCD19negCD56neg)
NK cells (total cells)
ICAM-1+ (mature neutros)
ICAM-1+ (activated neutros)
Neutrophils
CD5+ (CD19+)
CCR2+ (CD14+)
Monocytes (total cells)
CD11c+ (CD8+CD3+)
CD3+ (total cells)
Lymphocytes (FSC-SSC gate)
IgDnegCD27neg (CD19+)
iNKT (CD3+)
PD-1+ (CD4+CD3+)
CD1a+ (CD14+)
CD16hiCD15+ neutrophils
TCRγδ (CD3+)
Ratio CD4/CD8
CD11c+ (CD3negCD14negCD19negCD56neg)
CD19+ (total cells)
CD38+ (CD8+CD3+)
CD14hi CD16+ monocytes
CD38+ (neutrophils)
−log10 (P value)
3
2.5
2
1.5
1
0.5
0
Sex
Obesity
Thrombosis (comp)
Death
Invasive ventilation
Days × onset sxs
Days × PCR + Comorbidities (n)
Comp (n)
Comp: medical complication
sxs: symptoms
n: number
B
Severe SARS-CoV-2+ cases
CCR2+ (% CD14+)
P = 0.09
ICAM-1+ (% mature neutros)
ICAM-1+ (% activated neutros)
CD38+ (% CD8+)
P = 0.07
ALCAM+ (% CD14+)
P = 0.07
Survivor
Deceased
C
Days from PCR+ (d)
5
10
15
20
CCR2+ (% CD14+)
ICAM-1+ (% CD16hiCD15+CD11bhiCD62hi)
ICAM-1+ (% CD16hiCD15+CD11bhiCD62lo)
ALCAM+ (% CD14+)
NIH 5-8 Good outcome
NIH 1-4 Bad outcome
Frequencies
t0 t1 t2
CD38+ (% CD8+)
CD1a+ (% CD14+)
CD5+ (% CD19+)
PD-1+ (% CD4+)

Figure 7. Association between clinical parameters and longitudinal analysis of immune cell populations altered in SARS-CoV-2$^+$ patients. (**A**) Association between immune cell subsets and clinical parameters in SARS-CoV-2$^+$ patients as illustrated by heatmap and hierarchical clustering of the $-\log_{10}$(*P* value) analyzed by Mann-Whitney *U* test for categorical clinical parameters and by Spearman's correlation for continuous clinical parameters. (**B**) Proportions of different immune cell subsets among severe SARS-CoV-2$^+$ patients (severe COVID-19) according to survival at 60 days. Mann-Whitney *U* test was used. (**C**) Changes over time in frequencies of selected populations identified as specific to SARS-CoV-2$^+$, between baseline (t0), 24–72 hours (t1), and 4–7 days (t2). Size of dots reflects delay (in days) between first documented positive SARS-CoV-2 PCR to baseline sampling. Baseline samples were taken a median of 6 days (31/38 within 2- to 10-day interval) after first positive SARS-CoV-2 PCR. Generalized estimating equations analysis. Each symbol represents 1 patient. $^*P < 0.05$.

rophage responses in ARDS (66). As recently reviewed, further investigations will be necessary to elucidate whether B-1a depletion in SARS-CoV-2$^+$ patients facilitates aggressive inflammatory response and promotes lung damage (67).

We identified altered expression of cell adhesion molecules on peripheral immune cells from SARS-CoV-2$^+$ patients and an association of such changes with the outcome, including mortality, among patients with severe COVID-19 (Figures 6, 7B, and 8). We observed elevated ICAM-1$^+$ on mature and activated neutrophils in SARS-CoV-2$^+$ patients compared with their SARS-CoV-2$^-$ counterparts. Others have suggested that ICAM-1 is acquired by neutrophils as they exit the inflamed tissue to reenter the circulation (68). This process might contribute to the clearance of neutrophils from the site of injury (69) but can also participate in dissemination of inflammation and promotion of distant organ damage (44, 70). Furthermore, ICAM-1$^+$ neutrophils are associated with the formation of neutrophil extracellular traps (71, 72), which is a network of DNA, histone, and protein associated with thrombosis. Notably, an elevated ICAM-1$^+$ neutrophil subset was associated with the burden of medical complications (Figure 7A). We further found that ALCAM was present on an elevated proportion of monocytes, and to a lesser extent B cells, in SARS-CoV-2$^+$ individuals compared with other groups (Figures 4 and 6A). This elevated proportion of ALCAM$^+$ monocytes was associated with severe and fatal COVID-19 and persisted in cases with a bad outcome at 30 days. ALCAM is associated with transmigration of monocytes across pulmonary endothelium (73) and with T cell activation; it could therefore represent a relevant therapeutic target in COVID-19.

We detected significant and persistent alterations in the T cell compartment in SARS-CoV-2$^+$ patients compared with other groups. CD38$^+$CD8$^+$ T cells were more prominent in SARS-CoV-2$^+$ patients compared with other groups, especially in patients who experienced an unfavorable outcome and did not survive. It is possible that CD38$^+$CD8$^+$ T cells represent overactivated, potentially exhausted, and less efficient T cells in viral control, as suggested by HIV studies (74, 75). We observed an elevated proportion of T cells carrying PD-1 in both groups of hospitalized patients and higher levels in elderly patients (Figure 4). PD-1 expression on CD4$^+$ was more pronounced in SARS-CoV-2$^+$ patients and in patients who required a prolonged stay in the ICU (unfavorable outcome at 30 days). Whereas it is possible that PD-1 upregulation is a physiological attempt to limit immunopathology in the setting of immune hyperactivation and plays a positive role, taken together, our findings raise the question about the therapeutic potential of PD-1/PD-L1 pathway modulation to reverse immune exhaustion in SARS-CoV-2$^+$ patients, specifically in elderly patients (76–78). Notably, elderly patients with sepsis — particularly those with unfavorable prognosis — exhibit a prolonged lymphopenia, a preferential reduction of CD4$^+$ T cells, and elevated expression of PD-1 on CD4$^+$ and CD8$^+$ T cells (79–82). In animal models of sepsis, blockade of the PD-1/PD-L1 pathway restored T cell function and was associated with a decrease of the pathogen burden and better survival (78, 83–85). Whether such an approach will be beneficial in the context of COVID-19 will soon be determined by an ongoing phase II trial for treatment of patients infected with SARS-CoV-2 with an anti–PD-1 monoclonal antibody (ClinicalTrials.gov NCT04356508).

From a clinical point of view, the similarities uncovered between the immune profiles of SARS-CoV-2$^+$ and SARS-CoV-2$^-$ patients suggest that therapeutics targeting general nonspecific inflammatory processes could be tested in multiple severe acute illnesses when lymphopenia and neutrophilia are observed, especially in older patients. Some therapies successfully used in sepsis or other ICU care settings could be applied to COVID-19, as exemplified by the use of steroids in severe COVID-19 (86).

Our study has identified biomarkers specifically associated with an unfavorable outcome in COVID-19 patients. These surface markers could represent relevant potential therapeutic targets to explore in future studies, in particular PD-1 on CD4$^+$ T cells and ICAM-1 and ALCAM on neutrophils and antigen-presenting cells (B cells, monocytes). Finally, our longitudinal investigation has revealed markers that could predict a worse outcome and correlate with medical complications and mortality (Figures 7A and 8). We believe our experimental approach, whole blood staining and flow cytometry analysis, could be easily used in hospital diagnostic laboratories to follow patients over time and could complement other clinical follow-ups.

Methods

Cohort. Fifty SARS-CoV-2$^+$ patients and 22 SARS-CoV-2$^-$ patients admitted to the University of Montreal hospital center (CHUM) between April 7 and May 7, 2020, as well as 49 healthy controls from among CHUM personnel without known autoimmune/inflammatory or active infectious disease, were prospectively recruited to the study and included in the Biobanque Québécoise de la COVID-19 (BQC19). None of the patients included received an experimental treatment for COVID-19 (e.g., hydroxychloroquine, remdesivir, anti–IL-6) prior to peripheral blood sampling. One SARS-CoV-2$^+$ patient had to be excluded from analysis related to outcome and survival for participation after baseline sampling in an experimental pharmacological assay. SARS-CoV-2$^+$ and SARS-CoV-2$^-$ status was determined by PCR (repeated once when negative) among hospitalized patients. The absence of IgM or IgG antibodies against SARS-CoV-2 in the serum of SARS-CoV-2$^-$ hospitalized patients and of healthy controls was used to confirm the status of the donors. When possible, follow-up samples were obtained at 24–72 hours (t1) and at 4 to 8 days (t2) after the baseline sample (t0) for SARS-CoV-2$^+$ patients. A follow-up sample at 24–72 hours was obtained from 32 SARS-CoV-2$^+$ patients at 4–7 days from 28 patients and at both time points for 21

Immune cell population \ Association	Status ($CoV\text{-}2^+$ vs. $CoV\text{-}2^{neg}$)	Severity COVID-19 ($CoV\text{-}2^+$)	Outcome at 30 days ($CoV\text{-}2^+$)	Mortality at 60 days (severe $CoV\text{-}2^+$)
Neutrophils	↔	↑	↑	↗
Lymphocytes	↔	↓	↓	↘
$CD3^+$ T lymphocytes	↔	↓	↓	↘
$CD19^+$ B lymphocytes	↔	↔	↔	↔
Monocytes	↔	↓	↘	↓
NK cells	↔	↓	↓	↘
iNKT	↔	↔	↔	↔
TCRγδ	↔	↔	↔	↘
$PD\text{-}1^+$ $CD4^+$ T lymphocytes	↑	↔	↑	↔
$CD11c^+$ $CD8^+$ T lymphocytes	↓	↘	↔	↔
$CD38^+$ $CD8^+$ T lymphocytes	↑	↗	↑	↑
$CD27^{neg}IgD^{neg}$ B lymphocytes	↑	↔	↔	↔
$CD5^+CD19^+$	↘	↓	↘	↔
$CD16^{hi}CD15^+$ neutrophils	↔	↔	↔	↔
$CD123^+$ in $CD14^{neg}$ myeloid	↔	↘	↔	↘
$CD11c^+$ in $CD14^{neg}$ myeloid	↔	↔	↔	↔
$CD38^+$ promyelocytes	↑	↔	↔	↑
Mature neutrophils	↑	↔	↘	↔
$ICAM\text{-}1^+$ in mature and activated neutrophils	↗	↑	↑	↑
$CD14^{hi}CD16^+$ monocytes	↑	↔	↔	↓
$ALCAM^+$ monocytes	↑	↑	↗	↗
$CCR2^+$ monocytes	↓	↔	↓	↘
$CD1a^+$ monocytes	↑	↑	↗	↔

$CoV\text{-}2^+$: $SARS\text{-}CoV\text{-}2^+$; $CoV\text{-}2^{neg}$: $SARS\text{-}CoV\text{-}2^{neg}$

Figure 8. Summary of identified alterations in subsets of immune cells according to status, severity, outcome, and mortality. Red upward arrows indicate increased frequencies, green downward arrows decreased frequencies, and yellow bidirectional arrows similar frequencies of immune cells in the blood of $SARS\text{-}CoV\text{-}2^+$ versus $SARS\text{-}CoV\text{-}2^-$ patients in severe versus mild/moderate, in unfavorable versus good outcome, and in deceased patients versus survivors.

patients. For some subanalyses, patients were stratified according to age: younger than 60 years old versus 60 or older. Hospitalization in the ICU was used to define other severe acute illness in $SARS\text{-}CoV\text{-}2^-$ patients, and the need for high-flow or invasive ventilation in $SARS\text{-}CoV\text{-}2^+$ patients to was used to define severe COVID-19. In our cohort, 14/22 patients were classified as other severe acute illness and 21/50 as severe COVID-19. The 8-point NIH ordinal severity scale (ranging from 1 = death to 8 = discharged at home with no required care) was used to describe the outcome at 30 days. A score of 1 to 4 on the NIH scale was used to define an unfavorable or bad outcome; a score of 5 to 8 was used to define a favorable or good outcome at 30 days. Mortality up to 60 days after sampling was considered when indicated. Medical charts were reviewed by 2 independent physicians to collect clinical information.

Serological analyses. Levels of anti-Spike antibodies (flow cytometry), anti-RBD IgA, IgM, and IgG (ELISA), and the neutralization half-maximal inhibitory dilution (ID_{50}) of pseudoviral particles expressing the Spike from SARS-CoV-2 were performed as previously reported (32, 87) and detailed in Supplemental Methods. The seropositivity threshold was established with samples from 10 donors negative for COVID-19 (prepandemic), as previously described (32, 87).

Flow cytometry. Blood was obtained through venous puncture; collected in tubes containing trisodium citrate, citric acid, and dextrose (ACD); and processed within a median of 3.5 hours (maximum of 8.5 hours); 150 μL whole blood was used for each staining (3 stainings/sample, ref. 88). Three antibody panels were used, details of which are summarized in Supplemental Tables 2–4. Processing and acquisition of cells for flow cytometry analysis is detailed in Supplemental Methods.

Flow cytometry analysis. Flow cytometric data analysis was performed using FlowJo (version 10.6.2). Fluorescence-minus-one (FMO) controls and unstained samples were used to check the compensation matrices and determine positive populations. For both hypothesis-driven and data-driven analysis, doublets were excluded, and events were pregated on the FSC-A versus SSC-A biplot to define granulocytic, monocytic, and lymphocytic cell lineages based on size and granularity. Compensation matrices were calculated and applied. Data-driven analysis was performed on select cell lineages depending on the antibodies included in each panel: analysis of the first panel was performed on the events within the monocytic gate and the granulocytic gate, analysis of the second panel on the events within the monocytic gate and the lymphocytic gate, and analysis of the third panel on the events within the lymphocytic gate. Samples were then downsampled to an equal size and 1 large concatenated file was generated for each panel. Using the R packages flowCore 2.0.1 and FlowSOM 1.20.0 in R version 4.0.1, we applied the FlowSOM algorithm (22) on these concatenated files to create a FlowSOM map for each panel. In order to explore the relative proportion of clinically relevant immune cell populations, we used clustering strategies within broad FSC/SSC gates rather than on specific subpopulations. The modal value of clusters, as determined by the PhenoGraph clustering algorithm (21) in FlowJo on multiple random samples, was used to determine the number of clusters to input into FlowSOM. A heatmap of each panel's geometric MFI for each cellular cluster was generated with the R package pheatmap 1.0.12. UMAPs were generated using the R package UMAP 0.2.6.0.

Statistics. Analysis of frequency of populations and their association with SARS-CoV-2 status, severity, and outcome at 30 days were performed by Mann-Whitney *U* test (for factors with 2 categories) or by Kruskal-Wallis test (for factors with a number of categories >2) followed by Dunn's post hoc test. All tests were performed 2-sided, using a nominal significance threshold of *P* less than 0.05. For identification of populations of interest (Figures 2A and 4), nominal *P* values for Kruskal-Wallis tests were adjusted for multiple testing (adjusted *P* value) within each stain separately

using the method of Benjamini and Hochberg (89), which controls the FDR at a significance threshold we set at 0.05. Association between clinical categorical variables was assessed by Fisher's exact test. Correlation between continuous features was quantified by the Spearman's rank correlation. To assess frequencies of specific immune cell populations over time, longitudinal analysis was performed using generalized estimation equations as implemented in the R package gee using exchangeable correlation structure and including time as the fixed effect variable and patient ID as the random variable. Linear regression models were used to assess the confounding effect of age in the association between frequencies of immune cell subpopulations and HC versus SARS-CoV-2 status in younger individuals (<60 years old). The confounding effect was investigated by the change in the linear model's estimate for each subpopulation before and after adjusting for age.

Multivariate prediction of SARS-CoV-2$^+$, SARS-CoV-2$^-$, and HC status, using as candidate predictor variables the whole set of the immune subpopulations, was performed using random forest (54) classification models as implemented in the randomForest 4.6-14 R package using 1000 random trees and the default "mtry" (number of variables randomly sampled and tested in each node) parameter. A misclassification error for each status was calculated as the out-of-bag error by testing on the samples that were not randomly drawn at each tree generation. All statistical analyses were performed using the statistical package R version 4.0.1.

Study approval. This study was approved by the Comité d'éthique de la recherche du CHUM (CRCHUM) in accordance with the Declaration of Helsinki (IRB protocols 19.387 and 19.389). Written, informed consent was obtained for each patient and is detailed elsewhere (90).

Author contributions

CL, AP, DEK, NA, RMR, M Charabati, and CG designed the study and wrote the manuscript; the order of co–first authors was determined by flipping a coin. CL, AP, DEK, and NA supervised the study. AF, JFC, and NC provided scientific input for designing the study and writing the manuscript. RMR, M Charabati, RB, YCS, NF, APF, EG, HJ, FL, VAM, ACM, NB, AD, LB, SPA, GBB, M Benlarbi, M Boutin, JDD, RG, GG, AL, JP, JR, and KT performed experiments. CL, AFM, OT, RMR, M Charabati, and CG performed analysis. M Chassé, MD, and BL recruited patients for the study.

Acknowledgments

This study was funded by a grant from the CRCHUM foundation and by grant VR2-173203 from the Government of Canada through the COVID-19 Immunity Task Force in collaboration with the Canadian Institutes of Health Research. The BQC-19 is supported by the Fonds de recherche Québec-Santé (FRQS), Génome Québec, and the Public Health Agency of Canada. DEK is a FRQS Merit Research Scholar. NC, MD, and CL receive a FRQS salary award. AF and AP hold a Canada Research Chair. We acknowledge Dominique Gauchat and Philippe St-Onge from the CRCHUM flow cytometry platform for excellent technical guidance and support.

Address correspondence to: Catherine Larochelle, Department of Neuroscience, Université de Montréal, CRCHUM R09.424, 900 St-Denis Street, Montréal, Québec, Canada H2X 0A9. Phone: 514.890.8000 ext. 15370; Email: catherine.larochelle.chum@ssss.gouv.qc.ca.

1. Guan WJ, et al. Clinical characteristics of coronavirus disease 2019 in China. *N Engl J Med*. 2020;382(18):1708–1720.
2. Richardson S, et al. Presenting characteristics, comorbidities, and outcomes among 5700 patients hospitalized with COVID-19 in the New York City area. *JAMA*. 2020;323(20):2052–2059.
3. Petrilli CM, et al. Factors associated with hospital admission and critical illness among 5279 people with coronavirus disease 2019 in New York City: prospective cohort study. *BMJ*. 2020;369:m1966.
4. Williamson EJ, et al. Factors associated with COVID-19-related death using OpenSAFELY. *Nature*. 2020;584(7821):430–436.
5. Onder G, et al. Case-fatality rate and characteristics of patients dying in relation to COVID-19 in Italy. *JAMA*. 2020;323(18):1775–1776.
6. Wu Z, McGoogan JM. Characteristics of and important lessons from the coronavirus disease 2019 (COVID-19) outbreak in China: summary of a report of 72 314 cases from the Chinese Center for Disease Control and Prevention. *JAMA*. 2020;323(13):1239–1242.
7. Zhang B, et al. Clinical characteristics of 82 cases of death from COVID-19. *PLoS One*. 2020;15(7):e0235458.
8. Franceschi C, et al. Inflammaging: a new immune-metabolic viewpoint for age-related diseases. *Nat Rev Endocrinol*. 2018;14(10):576–590.
9. Aguilar EG, Murphy WJ. Obesity induced T cell dysfunction and implications for cancer immunotherapy. *Curr Opin Immunol*. 2018;51:181–186.
10. Bantug GR, et al. The spectrum of T cell metabolism in health and disease. *Nat Rev Immunol*. 2018;18(1):19–34.
11. Honce R, Schultz-Cherry S. Impact of obesity on influenza A virus pathogenesis, immune response, and evolution. *Front Immunol*. 2019;10:1071.
12. Keilich SR, et al. Diminished immune responses with aging predispose older adults to common and uncommon influenza complications. *Cell Immunol*. 2019;345:103992.
13. Rowe TA, McKoy JM. Sepsis in older adults. *Infect Dis Clin North Am*. 2017;31(4):731–742.
14. Mathew D, et al. Deep immune profiling of COVID-19 patients reveals distinct immunotypes with therapeutic implications. *Science*. 2020;369(6508):eabc8511.
15. Kuri-Cervantes L, et al. Comprehensive mapping of immune perturbations associated with severe COVID-19. *Sci Immunol*. 2020;5(49):eabd7114.
16. Diao B, et al. Reduction and functional exhaustion of T cells in patients with coronavirus disease 2019 (COVID-19). *Front Immunol*. 2020;11:827.
17. Pan F, et al. Factors associated with death outcome in patients with severe coronavirus disease-19 (COVID-19): a case-control study. *Int J Med Sci*. 2020;17(9):1281–1292.
18. Helms J, et al. Neurologic features in severe SARS-CoV-2 infection. *N Engl J Med*. 2020;382(23):2268–2270.
19. Bošnjak B, et al. Low serum neutralizing anti-SARS-CoV-2 S antibody levels in mildly affected COVID-19 convalescent patients revealed by two different detection methods. *Cell Mol Immunol*. 2021;18(4):936–944.
20. Weisberg SP, et al. Distinct antibody responses to SARS-CoV-2 in children and adults across the COVID-19 clinical spectrum. *Nat Immunol*. 2021;22(1):25–31.
21. Levine JH, et al. Data-driven phenotypic dissection of AML reveals progenitor-like cells that correlate with prognosis. *Cell*. 2015;162(1):184–197.
22. Van Gassen S, et al. FlowSOM: using self-organizing maps for visualization and interpretation of cytometry data. *Cytometry A*. 2015;87(7):636–645.
23. Zhou R, et al. Acute SARS-CoV-2 infection impairs dendritic cell and T cell responses. *Immunity*. 2020;53(4):864–877.
24. Leijte GP, et al. Monocytic HLA-DR expression kinetics in septic shock patients with different pathogens, sites of infection and adverse outcomes. *Crit Care*. 2020;24(1):110.
25. Remy KE, et al. Severe immunosuppression and not a cytokine storm characterizes COVID-19 infections. *JCI Insight*. 2020;5(17):140329.
26. Ziegler-Heitbrock L. The CD14$^+$ CD16$^+$ blood monocytes: their role in infection and inflammation. *J Leukoc Biol*. 2007;81(3):584–592.
27. Liu E, et al. Changes of CD14 and CD1a expres-

sion in response to IL-4 and granulocyte-macrophage colony-stimulating factor are different in cord blood and adult blood monocytes. *Pediatr Res*. 2001;50(2):184–189.
28. Sormani MP. An Italian programme for COVID-19 infection in multiple sclerosis. *Lancet Neurol*. 2020;19(6):481–482.
29. Ju B, et al. Human neutralizing antibodies elicited by SARS-CoV-2 infection. *Nature*. 2020;584(7819):115–119.
30. Liu L, et al. Potent neutralizing antibodies against multiple epitopes on SARS-CoV-2 spike. *Nature*. 2020;584(7821):450–456.
31. Gaebler C, et al. Evolution of antibody immunity to SARS-CoV-2 [preprint]. https://doi.org/10.1101/2020.11.03.367391. Posted on bioRxiv November 5, 2020.
32. Prévost J, et al. Cross-sectional evaluation of humoral responses against SARS-CoV-2 spike. *Cell Rep Med*. 2020;1(7):100126.
33. Morris G, et al. Emerging role of innate B1 cells in the pathophysiology of autoimmune and neuroimmune diseases: association with inflammation, oxidative and nitrosative stress and autoimmune responses. *Pharmacol Res*. 2019;148:104408.
34. Soldevila G, et al. The immunomodulatory properties of the CD5 lymphocyte receptor in health and disease. *Curr Opin Immunol*. 2011;23(3):310–318.
35. Gary-Gouy H, et al. Human CD5 promotes B-cell survival through stimulation of autocrine IL-10 production. *Blood*. 2002;100(13):4537–4543.
36. Rojas OL, et al. Characterization of rotavirus specific B cells and their relation with serological memory. *Virology*. 2008;380(2):234–242.
37. Colonna-Romano G, et al. A double-negative (IgD^-CD27^-) B cell population is increased in the peripheral blood of elderly people. *Mech Ageing Dev*. 2009;130(10):681–690.
38. Wei C, et al. A new population of cells lacking expression of CD27 represents a notable component of the B cell memory compartment in systemic lupus erythematosus. *J Immunol*. 2007;178(10):6624–6633.
39. Moir S, et al. Evidence for HIV-associated B cell exhaustion in a dysfunctional memory B cell compartment in HIV-infected viremic individuals. *J Exp Med*. 2008;205(8):1797–1805.
40. Glaría E, Valledor AF. Roles of CD38 in the immune response to infection. *Cells*. 2020;9(1):E228.
41. Jubel JM, et al. The role of PD-1 in acute and chronic infection. *Front Immunol*. 2020;11:487.
42. Filep JG, Ariel A. Neutrophil heterogeneity and fate in inflamed tissues: implications for the resolution of inflammation. *Am J Physiol Cell Physiol*. 2020;319(3):C510–C532.
43. Nourshargh S, Alon R. Leukocyte migration into inflamed tissues. *Immunity*. 2014;41(5):694–707.
44. Woodfin A, et al. ICAM-1-expressing neutrophils exhibit enhanced effector functions in murine models of endotoxemia. *Blood*. 2016;127(7):898–907.
45. Filippi M-D. Neutrophil transendothelial migration: updates and new perspectives. *Blood*. 2019;133(20):2149–2158.
46. Wang JH, et al. Intercellular adhesion molecule-1 (ICAM-1) is expressed on human neutrophils and is essential for neutrophil adherence and aggregation. *Shock*. 1997;8(5):357–361.
47. Takashi S, et al. Contribution of CD54 to human eosinophil and neutrophil superoxide production. *J Appl Physiol (1985)*. 2001;91(2):613–622.
48. Zimmerman AW, et al. Long-term engagement of CD6 and ALCAM is essential for T-cell proliferation induced by dendritic cells. *Blood*. 2006;107(8):3212–3220.
49. Golinski M-L, et al. $CD11c^+$ B cells are mainly memory cells, precursors of antibody secreting cells in healthy donors. *Front Immunol*. 2020;11:32.
50. Maus UA, et al. CCR2-positive monocytes recruited to inflamed lungs downregulate local CCL2 chemokine levels. *Am J Physiol Lung Cell Mol Physiol*. 2005;288(2):L350–L358.
51. Merad M, Martin JC. Pathological inflammation in patients with COVID-19: a key role for monocytes and macrophages. *Nat Rev Immunol*. 2020;20(6):355–362.
52. Beyer M, et al. The beta2 integrin CD11c distinguishes a subset of cytotoxic pulmonary T cells with potent antiviral effects in vitro and in vivo. *Respir Res*. 2005;6(1):70.
53. Vinay DS, et al. Origins and functional basis of regulatory $CD11c^+CD8^+$ T cells. *Eur J Immunol*. 2009;39(6):1552–1563.
54. Breiman L. Random forests. *Mach Learn*. 2001;45(1):5–32.
55. Liang KY, Zeger SL. Longitudinal data analysis using generalized linear models. *Biometrika*. 1986;73(1):13–22.
56. Wang F, et al. Characteristics of peripheral lymphocyte subset alteration in COVID-19 pneumonia. *J Infect Dis*. 2020;221(11):1762–1769.
57. Laing AG, et al. A dynamic COVID-19 immune signature includes associations with poor prognosis. *Nat Med*. 2020;26(10):1623–1635.
58. Duggal NA, et al. Innate and adaptive immune dysregulation in critically ill ICU patients. *Sci Rep*. 2018;8(1):10186.
59. Sokolowska M, et al. Immunology of COVID-19: mechanisms, clinical outcome, diagnostics, and perspectives-A report of the European Academy of Allergy and Clinical Immunology (EAACI). *Allergy*. 2020;75(10):2445–2476.
60. Stefania V, et al. Unique immunological profile in patients with COVID-19. *Cell Mol Immunol*. 2021;18(3):604–612.
61. Zahorec R. Ratio of neutrophil to lymphocyte counts — rapid and simple parameter of systemic inflammation and stress in critically ill. *Bratisl Lek Listy*. 2001;102(1):5–14.
62. Al-Amodi O, et al. CD1a-expressing monocytes as mediators of inflammation in ulcerative colitis. *Inflamm Bowel Dis*. 2018;24(6):1225–1236.
63. Monserrat J, et al. Early alterations of B cells in patients with septic shock. *Crit Care*. 2013;17(3):R105–R.
64. Wen W, et al. Immune cell profiling of COVID-19 patients in the recovery stage by single-cell sequencing. *Cell Discov*. 2020;6:31.
65. Aziz M, et al. B-1a cells protect mice from sepsis: critical role of CREB. *J Immunol*. 2017;199(2):750–760.
66. Aziz M, et al. B-1a cells protect mice from sepsis-induced acute lung injury. *Mol Med*. 2018;24(1):26.
67. Aziz M, et al. Therapeutic potential of B-1a cells in COVID-19. *Shock*. 2020;54(5):586–594.
68. Buckley CD, et al. Identification of a phenotypically and functionally distinct population of long-lived neutrophils in a model of reverse endothelial migration. *J Leukoc Biol*. 2006;79(2):303–311.
69. Mathias JR, et al. Resolution of inflammation by retrograde chemotaxis of neutrophils in transgenic zebrafish. *J Leukoc Biol*. 2006;80(6):1281–1288.
70. Colom B, et al. Leukotriene B4-neutrophil elastase axis drives neutrophil reverse transendothelial cell migration in vivo. *Immunity*. 2015;42(6):1075–1086.
71. Folco EJ, et al. Neutrophil extracellular traps induce endothelial cell activation and tissue factor production through interleukin-1α and cathepsin G. *Arterioscler Thromb Vasc Biol*. 2018;38(8):1901–1912.
72. Ode Y, et al. CIRP increases $ICAM\text{-}1^+$ phenotype of neutrophils exhibiting elevated iNOS and NETs in sepsis. *J Leukoc Biol*. 2018;103(4):693–707.
73. Masedunskas A, et al. Activated leukocyte cell adhesion molecule is a component of the endothelial junction involved in transendothelial monocyte migration. *FEBS Lett*. 2006;580(11):2637–2645.
74. Hua S, et al. Potential role for HIV-specific $CD38^-$ /$HLA\text{-}DR^+$ $CD8^+$ T cells in viral suppression and cytotoxicity in HIV controllers. *PLoS One*. 2014;9(7):e101920.
75. Taborda NA, et al. Higher frequency of NK and $CD4^+$ T-cells in mucosa and potent cytotoxic response in HIV controllers. *PLoS One*. 2015;10(8):e0136292.
76. Saeidi A, et al. T-cell exhaustion in chronic infections: reversing the state of exhaustion and reinvigorating optimal protective immune responses. *Front Immunol*. 2018;9:2569.
77. Chang K, et al. Targeting the programmed cell death 1: programmed cell death ligand 1 pathway reverses T cell exhaustion in patients with sepsis. *Crit Care*. 2014;18(1):R3.
78. Brahmamdam P, et al. Delayed administration of anti-PD-1 antibody reverses immune dysfunction and improves survival during sepsis. *J Leukoc Biol*. 2010;88(2):233–240.
79. Inoue S, et al. Reduction of immunocompetent T cells followed by prolonged lymphopenia in severe sepsis in the elderly. *Crit Care Med*. 2013;41(3):810–819.
80. Guignant C, et al. Programmed death-1 levels correlate with increased mortality, nosocomial infection and immune dysfunctions in septic shock patients. *Crit Care*. 2011;15(2):R99.
81. Zhang Y, et al. Upregulation of programmed death-1 on T cells and programmed death ligand-1 on monocytes in septic shock patients. *Crit Care*. 2011;15(1):R70.
82. Patera AC, et al. Frontline Science: defects in immune function in patients with sepsis are associated with PD-1 or PD-L1 expression and can be restored by antibodies targeting PD-1 or PD-L1. *J Leukoc Biol*. 2016;100(6):1239–1254.
83. Zhang Y, et al. PD-L1 blockade improves survival in experimental sepsis by inhibiting lymphocyte

apoptosis and reversing monocyte dysfunction. *Crit Care*. 2010;14(6):R220.
84. Busch LM, et al. Checkpoint inhibitor therapy in preclinical sepsis models: a systematic review and meta-analysis. *Intensive Care Med Exp*. 2020;8(1):7.
85. Chang KC, et al. Blockade of the negative co-stimulatory molecules PD-1 and CTLA-4 improves survival in primary and secondary fungal sepsis. *Crit Care*. 2013;17(3):R85.
86. Prescott HC, Rice TW. Corticosteroids in COVID-19 ARDS: evidence and hope during the pandemic. *JAMA*. 2020;324(13):1292–1295.
87. Beaudoin-Bussières G, et al. Decline of humoral responses against SARS-CoV-2 spike in convalescent individuals. *mBio*. 2020;11(5):e02590–20.
88. Shankey TV, et al. An optimized whole blood method for flow cytometric measurement of ZAP-70 protein expression in chronic lymphocytic leukemia. *Cytometry B Clin Cytom*. 2006;70(4):259–269.
89. Benjamini Y, Hochberg Y. Controlling the false discovery rate: a practical and powerful approach to multiple testing. *J R Stat Soc Series B Stat Methodol*. 1995;57(1):289–300.
90. Knoppers BM, et al. Modeling consent in the time of COVID-19. *J Law Biosci*. 2020;7(1):lsaa020.